

**PUBLICATIONS OF THE ASTRONOMICAL INSTITUTE OF  
THE UNIVERSITY OF AMSTERDAM**

---

No. 9

**A. PANNEKOEK and D. KOELBLOED**

**PHOTOGRAPHIC PHOTOMETRY  
OF THE SOUTHERN MILKY WAY**

after negatives chiefly taken at the Bosscha

Observatory at Lembang by

**DR. J. G. E. G. VOÛTE**

---

**AMSTERDAM – STADSDRUKKERIJ – 1949**



## TABLE OF CONTENTS.

1. Plan of the work . . . . .	1
2. Instruments and program . . . . .	1
3. The measurements . . . . .	4
4. Derivation of reduction curves . . . . .	5
5. The extrafocal stardiscs . . . . .	8
6. The linear scale of the plates . . . . .	10
7. The intensity distribution across the stardiscs . . . . .	11
8. The limiting magnitude of the stars . . . . .	13
9. Reduction formulae for surface brightness . . . . .	13
10. Reduction to the centre of the plate . . . . .	15
11. Reduction of the intensities to one system . . . . .	22
12. The final results . . . . .	26

Plate I. Reproductions of four Lembang plates.

Plate II and III. Drawings in shades of galactic regions between  $309^{\circ}$ — $340^{\circ}$  and  $339^{\circ}$ — $10^{\circ}$  longitude.

Charts I—XV. Isophotic charts with mean intensity values.



## 1. PLAN OF THE WORK.

In No. 3 of these Publications the results of a photometry of the Northern Milky Way, based on extrafocal photographs taken by Max Wolf at Heidelberg and measured at the Amsterdam Institute, were published. The promising results of the measurements of the first plates among them immediately aroused the desire to extend this method to the southern half of the Milky Way. In 1926, the first author stayed at the Bosscha Observatory at Lembang for a visual study of the Southern Milky Way. On this occasion experiments were made with a newly acquired set of two wide angle camera objectives, with angular apertures 1 : 3.5 and 1 : 2.7. As they appeared to be successful, the plan was made to have a regular series of extrafocal photographs covering the entire southern galactic zone taken at Lembang with the latter of these cameras, to be afterwards measured at Amsterdam. Since the angular aperture was larger than that of the Heidelberg instrument, the necessary exposure time was less, but the usable field was smaller, so that a greater number of plates was required to cover the entire area. As a result of our first experiments the exposure time was fixed at one hour; in later years this was increased to 75 minutes.

The completion of the program has met with many difficulties. Because the same instrument had to be used for other purposes also, especially in variable star work, the regular progress of the Milky Way plates was repeatedly interrupted. A number of plates were of less good quality, so that it was decided to have them re-taken. In the same way it was deemed advisable to repeat a few exposures when the star discs were too small. So up to the last, gaps in the program had to be filled up. Since the most southern part of the Milky Way could not well be taken at the low southern latitude of  $6^{\circ}.8$  of Lembang, the original plan was that after finishing the plates at Lembang, the instrument should be sent to a station farther south, in order that the southernmost plates could be taken there. As the completion of the Lembang plates was protracted because the instrument was needed for other work, Dr. Voûte planned to take the camera with him to South Africa after his retirement, to make there the remaining exposures himself. But the war interfered with the plan. Then at my request Dr. Shapley kindly offered in 1940 to have the missing plates taken with a similar instrument at the Boyden station of Harvard College Observatory at Mazelspoort in South Africa (latitude  $29^{\circ}.2$  South), and the necessary preparations were made. But soon the extension of the war prevented any further communication. So finishing the program had to be put off till these communications had been restored after the war. In 1945 we received 10 plates taken by Dr. J. S. Paraskevopoulos in 1942, with an exposure time of three hours. Two of these plates had to be rejected and were repeated in 1946. We are highly indebted to Dr. Shapley and Dr. Paraskevopoulos for having enabled us in this way to carry our work to completion.

## 2. INSTRUMENTS AND PROGRAM.

The camera used at Lembang for the extrafocal Milky Way plates, indicated by B, has a Zeiss Tessar of 53.5 mm aperture and 145 mm focal distance. It was attached, together with a Zeiss Triotar for focal exposures, at the Zeiss 13 cm refractor of the Lembang Observatory, provided with a driving clock (cf. Description of the Observatory <sup>1)</sup>). No guiding was needed after the central star had been set in the refractor; only now and then its position on the cross wire was checked and when necessary, corrected. Since the field of the refractor is small, mistakes in identification sometimes occurred. The amount that the plateholder was put out of focus was read by means of a scale attached to the tube.

The camera lens used at the Boyden station, a Ross London Patent Xpress, had an aperture of  $1\frac{1}{2}$  inch; with its smaller angular aperture of 1 : 4 the exposure time had to be longer than with the Lembang instrument.

<sup>1)</sup> Annalen v. d. Bosscha Sterrenwacht I.A. p. 26. Plate XI.

To cover the galactic zone in a regular way central stars were chosen as near as possible to points at latitudes  $0^\circ$ ,  $+10^\circ$ ,  $-10^\circ$  (after Marth's galactic coordinates <sup>1)</sup> based on the position of the galactic pole  $12^h 40^m, +30^\circ$ , with  $10^\circ$  interval in longitude, at longitudes  $180^\circ$ ,  $190^\circ \dots$  for latitude  $0^\circ$ , and at alternating longitudes  $175^\circ$ ,  $185^\circ \dots$  for latitudes  $\pm 10^\circ$ . In some regions with interesting structures at high latitudes (Orion, Scorpio) a few plates with central stars at  $+20^\circ$  or  $-20^\circ$  latitude were added. For some plates the centre is off owing to a wrong identification of the central star. If the distance was great the plate was repeated and the first plate was considered as an additional plate and was also measured (in table 1 they are indicated by letters A—F). When, in the case of a wrong centre, the exposure was not repeated, an asterisk is added to the number in table 1. The addition of two asterisks denotes a Boyden-plate with the same centre as a Lembang-plate already measured. The fields are indicated in regular sequence of longitude by P 1 to P 65. Table 1 gives, in chronological order, a list of the plates measured and used in the discussions. There are 63 Lembang-plates to which afterwards 10 Boyden-plates were added.

TABLE 1. LIST OF PLATES USED (Plates taken at Lembang).

Plate Nr.	Field Nr.	Centre (1880)	Gal. Coord.	Centr. Star	Date	Mid Java Time		Expos.
		h m °				h m	h m	
B 30	52	17 40 — 27.8	328.8 — 2.0	X Sgr	11. 6. 26			60
„ 32	45A	16 46 — 42.2	310.7 — 1.7	ζ Sco	12. 6. 26			60
„ 34	50	18 9 — 36.8	324.2 — 12.0	η Sgr	12. 6. 26	13 5 — 14 5		60
„ 38	52D	17 19 — 24.1	329.2 + 4.0	b Oph	13. 6. 26			65
„ 40	35C	14 12 — 55.8	282.7 + 2.0	V Cen	14. 6. 26			60
„ 42	46	17 29 — 42.9	314.8 — 8.4	ϑ Sco	14. 6. 26			60
„ 44	41	15 54 — 48.9	299.5 — 0.0	η Nor	14. 6. 26	12 0 — 13 7		67
„ 46	51	16 50 — 23.0	326.0 + 10.0	24 Oph	14. 6. 26	12 48 — 13 50		62
„ 48	42	16 54 — 53.1	303.0 — 9.6	ε <sub>2</sub> Ara	15. 6. 26	10 27 — 11 27		60
„ 98	25	10 27 — 44.5	246.6 + 9.6	s Vel	2. 2. 27	15 15 — 16 15		60
„ 104	34	13 0 — 49.3	273.3 + 10.6	ξ <sub>2</sub> Cen	1. 3. 27	15 35 — 16 35		60
„ 110	36	15 26 — 65.9	286.0 — 11.0	ε TrA	2. 3. 27	14 30 — 15 30		60
„ 128	52E	17 40 — 27.8	328.8 — 2.0	X Sgr	7. 7. 27	14 15 — 15 15		60
„ 130	64*	19 31 — 1.6	5.0 — 11.7	ι Aql	7. 7. 27	15 30 — 16 30		60
„ 227	30	12 2 — 50.1	263.8 + 9.5	δ Cen	19. 1. 29	15 16 — 16 16		60
„ 233	5	5 42 — 9.7	181.4 — 17.3	κ Ori	3. 2. 29	9 15 — 10 15		60
„ 235	3	5 53 + 0.5	173.5 — 10.0	60 Ori	3. 2. 29	10 30 — 11 30		60
„ 237	8F	6 41 — 10.0	188.8 — 4.8	75 Mon	3. 2. 29	11 45 — 12 45		60
„ 239	9	6 33 — 18.1	195.0 — 10.5	ν <sub>3</sub> CMa	3. 2. 29	13 0 — 14 0		60
„ 241	20*	9 4 — 42.9	233.6 + 1.8	λ Vel	17. 2. 29	13 55 — 14 55		60
„ 243	31	11 44 — 69.6	265.1 — 10.1	17 Mus	13. 5. 29			60
„ 245	6	6 14 — 7.8	183.5 — 9.5	7 Mon	12. 9. 29	15 42 — 16 42		60
„ 261	13	6 57 — 27.8	206.3 — 10.2	σ CMa	28. 9. 29	16 16 — 17 16		60
„ 2333	43	15 35 — 37.0	304.2 + 11.4	h Lup	18. 4. 33	13 0 — 14 0		60
„ 2335	53	16 31 — 10.3	333.3 + 21.5	ζ Oph	18. 4. 33	14 15 — 15 15		60
„ 2339	48	16 0 — 20.5	319.9 + 20.2	ω <sub>2</sub> Sco	19. 4. 33	14 42 — 15 42		60
„ 2340	47	16 17 — 29.4	316.1 + 11.2	67 Sco	19. 4. 33	15 51 — 16 51		60
„ 2343	38	15 2 — 54.9	289.5 — 0.2	59 Lup	20. 4. 33	12 45 — 13 45		60
„ 2344	49	17 7 — 33.4	320.1 + 0.5	134 Sco	20. 4. 33	14 0 — 15 0		60
„ 2347	54	17 4 — 15.6	334.0 + 11.9	η Oph	20. 4. 33	15 32 — 16 32		60
„ 2349	55	18 21 — 25.5	335.5 — 8.6	λ Sgr	21. 4. 33	13 28 — 14 28		60
„ 2361	60	17 56 + 1.3	355.6 + 10.2	68 Oph	23. 4. 33	13 55 — 14 55		60
„ 2363	63	18 2 + 9.5	3.6 + 13.0	72 Oph	23. 4. 33	15 2 — 16 2		60
„ 2364	61	19 6 — 8.1	356.2 — 9.7	20 Agl	23. 4. 33	16 8 — 17 8		60
„ 2370	59*	18 22 — 14.6	345.1 — 3.5	2 H Sct	24. 4. 33	14 52 — 15 52		60

<sup>1)</sup> A. Marth, M.N. 53, 74, 384 (1893).

Plate Nr.	Field Nr.	Centre (1880)	Gal. Coord.	Centr. Star	Date	Mid Java Time	Expos.
		h m °				h m h m	m
B 2404	14	7 44 — 24.6	209.1 + 0.6	ξ Pup	27. 4. 33	7 5 — 8 5	60
„ 2414	18	9 5 — 29.9	224.5 + 11.2	ε Pyx	27. 4. 33	8 12 — 9 12	60
„ 2420	26	10 16 — 55.4	250.6 — 0.8	J Vel	27. 4. 33	10 35 — 11 35	60
„ 2427	16	8 33 — 25.8	216.6 + 8.6	η Pyx	27. 4. 33	7 3 — 8 3	60
„ 2433	50	18 9 — 36.8	324.2 — 12.0	η Sgr	4. 5. 33	15 55 — 16 55	60
„ 2442	37	14 12 — 45.5	286.2 + 11.7	ι Lup	22. 5. 33	8 32 — 9 32	60
„ 2443	40	15 5 — 44.0	295.4 + 8.9	e Lup	22. 5. 33	10 45 — 11 45	60
„ 2447	32	12 41 — 59.0	270.1 + 1.0	β Cru	23. 5. 33	9 30 — 10 30	60
„ 2451	45B	17 4 — 43.1	312.0 — 4.8	η Sco	24. 5. 33	15 20 — 16 20	60
„ 2460	21*	8 23 — 51.3	235.2 — 9.0	28 Vel	25. 5. 33	6 55 — 7 55	60
„ 2462	23	9 44 — 36.6	234.8 + 12.5	31 Ant	25. 5. 33	8 15 — 9 15	60
„ 3245	2	6 57 + 11.1	172.4 + 9.2	BAC 2306	25. 11. 38	12 30 — 13 45	75
„ 3246	4	6 42 + 2.5	178.0 + 1.6	18 Mon	25. 11. 38	14 5 — 15 20	75
„ 3247	7	7 26 + 2.2	183.9 + 11.0	δ <sub>1</sub> CMi	25. 11. 38	15 25 — 16 40	75
„ 3247a	8	6 55 — 8.2	189.0 — 1.0	101 Mon	26. 11. 38	13 25 — 14 40	75
„ 3248	10	7 44 — 8.9	195.9 + 9.2	154 Mon	21. 12. 38	13 45 — 15 0	75
„ 3249	11	7 22 — 17.6	200.4 — 0.1	176 CMa	15. 1. 39	12 50 — 14 5	75
„ 3250	12	8 8 — 15.4	204.7 + 10.3	269 Pup	15. 1. 39	14 10 — 15 25	75
„ 3251	22	9 33 — 48.8	241.3 + 0.8	M Vel	15. 1. 39	15 28 — 16 28	60
„ 3252	27	11 7 — 48.4	254.7 + 8.8	9 Cen	19. 1. 39	13 45 — 14 50	65
„ 3253	17	8 9 — 35.5	221.1 — 1.4	r Pup	20. 1. 39	10 25 — 11 22	57
„ 3254	19	7 39 — 44.9	225.7 — 11.3	159 Pup	20. 1. 39	12 10 — 11 5	55
„ 3255	1	5 16 — 0.5	169.6 — 18.4	22 Ori	11. 2. 39	10 33 — 11 48	75
„ 3256	24	9 8 — 58.5	245.0 — 8.9	a Car	11. 2. 39	11 52 — 13 7	75
„ 3260	44	15 30 — 27.7	309.3 + 19.5	v Lib	23. 5. 39	9 40 — 10 55	75
„ 3261	57	17 31 — 8.0	344.2 + 10.6	μ Oph	23. 5. 39	12 0 — 13 15	75
„ 3262	56	18 1 — 17.2	340.3 — 0.4	32 Sgr	23. 5. 39	12 20 — 13 35	75
„ 3263	58	18 48 — 18.2	344.8 — 11.0	117 Sgr	23. 5. 39	13 45 — 15 0	75
„ 3264	62	18 40 — 1.1	359.1 — 0.6	5 Aql	24. 5. 39	13 48 — 15 3	75
„ 3265	65	18 50 + 4.0	4.8 — 0.2	δ Ser	24. 5. 39	15 20 — 16 35	75

(Plates taken at the Boyden-Station).

Plate Nr.	Field Nr.	Centre (1880)	Gal. coord	Centr. Star	Date	Sideral Time of exposure	Expos.
		h m °					m
193	24**	9 8 — 58.5	245.0 — 8.9	a Car	13. 1. 42	5 10 — 8 10	180
194	15	7 13 — 36.9	216.1 — 11.6	π Pup	20. 1. 42	4 1 — 7 1	180
197	28	10 10 — 65.8	255.3 — 10.0	M Car	8. 3. 42	6 30 — 9 30	180
201	36**	15 25 — 65.9	286.0 — 11.0	ε TrA	16. 3. 42	12 27 — 15 27	180
205	29	11 46 — 64.5	264.2 — 5.1	18 Mus	22. 3. 42	11 43 — 14 43	180
207	32**	12 41 — 59.0	270.1 + 1.0	β Cru	24. 3. 42	11 20 — 14 20	180
209	39	16 20 — 61.4	293.6 — 11.6	33 TrA	25. 3. 42	14 24 — 17 24	180
235	35	13 55 — 59.8	279.4 — 1.1	β Cen	23. 4. 42	13 53 — 16 53	180
2476	31**	11 44 — 69.6	265.1 — 10.1	17 Mus	30. 1. 46	7 15 — 10 15	180
2479	33	13 17 — 70.0	273.2 — 10.2	67 Mus	3. 3. 46	9 17 — 12 17	180

The plan of the work and its program was devised by A. Pannekoek who is also responsible for the final drawing of the isophotes, whereas D. Koelbloed has made all the measurements and reductions as well as their discussion and the derivation of the intensity values.

### 3. THE MEASUREMENTS.

The Milky Way phenomenon is a variation of surface brightness across the sky, produced by the different distribution of telescopic stars, which cannot be seen separately but whose combined light falling upon the retina elements gives the impression of a continuous surface illumination. A photographic plate depicts these stars as separate points, with the exception of the closely packed stars of the faintest classes, which merge into continuous mottled masses of cloud form. The pictorial effect of the cloudforms in Milky Way photographs is an effect of exaggeration; it is due to the fact, that a number of closely packed black star-images presents a stronger image than does one single star of their combined brightness, as can be easily seen e.g. in the clusters on the Franklin-Adams maps. In order to get a real Milky Way representation, a blackening of the plate representing the true surface brightness, we have to set the plate out of focus, so that each star spreads its light over a disc of certain size. Each point of the plate then receives per unit area the average light per unit area of all the stars contained within the extrafocal disc around this point; this total brightness per unit area determines the density of the silver deposit at that point. The discs of the brighter stars only, above a certain limit, emerge from this smooth mass as separate objects. It cannot be said beforehand what that limit will be; the larger the discs, the smaller the number of brightest stars that can be seen separately, whereas all the fainter ones contribute to the background intensity. If we could choose the dimensions of the stellar discs in such a way that the limit were  $6^m.5$ , the picture, but for the large stellar discs, would resemble the visual aspect of the Milky Way. On the Heidelberg-plates of the Northern Milky Way this limiting magnitude was found to be 7.5 to 8.5. Since the contribution of the 7<sup>th</sup> and 8<sup>th</sup> magnitude stars to the galactic light is very slight, the difference is negligible. Moreover using the measured surface brightness for determining stellar distributions this limiting magnitude is quite as good as any other one. For the sake of homogeneity we have kept as much as possible the same conditions in the present investigation of the Southern Milky Way, in particular the apparent size of the stellar disc.

For the derivation of the surface brightness of the sky at a great number of points, we have to measure first the density of the silver deposit at these points on the photographic plates, and then to derive the relation between this density (the blackness) and the surface brightness producing it.

The way in which the density is measured by means of the Hartmann-microphotometer of the Institute has been described in detail in the former Northern work (Amst. Publ. 3, p. 4—6). In this instrument the image of a small circular portion of 0.3 mm diameter of the plate is viewed together with the surrounding image of a movable obscuring wedge; the wedge reading in case of equality is transformed into a linear scale of blackening; 1 mm corresponds to 10 units of blackening. On each plate the points were measured in parallel rows 1 mm apart. In the former work the distance between successive points of each row was 2 mm, and the points in successive rows alternated diamondwise. In the present work the same arrangement (giving 1 point per 2 sq.mm) was followed in the fainter and outlying parts. In the rich regions, however, of Sagittarius, Scorpio and Centaurus where rapid variations occur over small distances, a double number of points was measured, so that they followed one another at a 1 mm interval in each row. Only a small number of rows could be measured in one hour; the small systematic differences between different sets of readings due to personal disposition and slight differences in adjustment of the apparatus were determined by separate comparison series, and so for the entire plate the results could be brought into one homogeneous system.

Plate I gives a reproduction of four of the Lembang plates at an enlarged scale ( $1.35 \times$ ). The exposed field on the negatives has a diameter of about 80 mm. On account of strong distortion of the stellar discs towards the edge of the plate, it was only possible to measure the central portion contained within a radius of 25 mm. In the Heidelberg plates used for the Northern Milky Way this distortion was much less pronounced and a square of 60 mm side was measured; in the present work it was not deemed advisable to go beyond a circle of 50 mm diameter for the Lembang plates, whereas 60 mm was measured on the Boyden-plates.



A considerable number of these regular points fell on visible stardisks and had to be omitted from measurement. In such cases small open spaces between the star discs were measured; their coordinates were read to 0.1 mm. Where many bright telescopic stars are crowded large gaps may occur in the rows which produce blank spaces without data on the maps.

From the measured blackening at a certain point we had to subtract the blackening for the unexposed border parties of the plate due to chemical and other fog, to the absorption of the glass and the dead film; the difference  $s$  is the silverdensity produced by the illumination.

In order to find the relation between the density  $s$  and the illumination by which it is produced, we make use of the discs of the stars which are separately visible. For all these stars the centre of the disc, where it was free from other overlapping discs, was measured in the same way as the points outside. The density here is produced by the background increased by the light of the star itself. The surface brightness due to the star may be calculated from its magnitude, the diameter of the disc and the distribution of light over the disc, and is expressed in the unit of one  $10^m$  star per square degree. From a number of brighter and fainter stars, reduction curves to derive the intensity from the measured density were deduced.

#### 4. DERIVATION OF REDUCTION CURVES.

For every plate the rectangular coordinates of the centres of all the visible stars were read, whether their blackening was measured or not. The latter was the case if the discs overlapped. These position readings were used to construct a map of them. To identify these stars it was compared with a map drawn after the Henry Draper Catalogue (Harvard Annals 90—99), with the photographic magnitude indicated for each star. The photographic magnitudes for stars south of  $-19^\circ$  as given in this catalogue had been derived from the Cape Durchmusterung by first reducing them to a standard scale. These magnitudes, however, could not be used owing to their large errors. Also the reduction of the Cape magnitudes by Halm and Spencer Jones <sup>1)</sup> appeared to give unsatisfactory results. Hence the photographic magnitudes were derived by adding the color index as given by the spectral class, to the photometric magnitude in the same catalogue.

The relation between the density  $s$  and the intensity  $h$  of the light producing it, is expressed by the characteristic curve. This intensity consists of the background intensity  $h_0$  and the intensity  $h$  due to the star. If we suppose for a moment that  $h_0$  is constant over the plate, then a certain density  $s_0$  corresponds to it. The part of the characteristic curve below the point  $(s_0, h_0)$  cannot be found because  $h_0$  is unknown and lower intensities do not occur on the plate. We can only plot  $s-s_0$  against  $h$  for the stars of different brightness, and this is then used in first approximation for the characteristic curve  $s$  against  $h$ . Now the background intensity  $h_0$  varies over the plate because it fluctuates over the galactic clouds and moreover decreases with increasing distance from the centre. So  $(s_0, h_0)$  does not represent one point but a certain portion of the true characteristic curve. For every star we have to take its proper  $s_0$  derived from the measures in its surroundings.

This was the procedure followed in the previous work in Publ. 3. The light of each star  $H$  (which is proportional to  $h$ ) expressed as number of  $10^m$  stars was plotted against  $s-s_0$ , and represented by a quadratic expression

$$H = a(s-s_0) + b(s-s_0)^2.$$

Here  $s_0$  represents a certain average background value for all the stars used. The fluctuations in this background, which express the variations in Milky Way intensity, are now found by the same expression  $H = as + b(s-s_0)^2$ , where by the omission of  $as_0$  and our ignorance as to the lower part of the curve, the resulting values contain an unknown amount, constant for each plate. By means of a proper factor, by which the coefficients  $a$  and  $b$  are multiplied, the stellar intensity  $H$  is converted into surface intensity  $h$ .

<sup>1)</sup> H. Spencer Jones: Magnitudes of stars contained in the Cape Zone Catalogue, 1927.

The same procedure was followed for most of the southern plates, without encountering difficulties. In the case of regions with bright galactic features, however, large differences occurred for stars on a bright background for the intensity read off the thus obtained characteristic curve and the original  $H$ . So in this case another method was followed afterwards, by working not with  $s-s_0$  but with  $s$  and  $s_0$  themselves. From the smaller values of  $s$  and  $s_0$  the lower linear part of the curve was constructed; then for each larger value  $s_0$  within this part the corresponding  $H_0$  was read and added to the stellar value  $H$ ; the sum total  $H_0 + H$  with  $s$  gave a higher point of the curve. In this way the entire curve could be built up. The differences with the former curves were only important for bright stars on a bright background, but for the part of the curve needed for the galactic intensities they were unimportant.

For the faintest stars selection effects may vitiate the figure of the curve. The very lowest part of the characteristic curve can best be found by making use of the condition:  $s-s_0 = 0$ ,  $H = 0$ , by definition, and for this reason all the small values, mostly below  $s-s_0 = 10$  were excluded. The other data were grouped in averages of  $s-s_0$  and of  $H$ . In Table 2a the data, used for derivation of the constants  $a$  and  $b$  of the expressions for  $H$  are given for plate B 3255 (Field 1) as an example for the remaining intensity differences. The first two columns contain the averages of  $s-s_0$  and  $H$ ; the large values below the horizontal lines have not been used in the computation. The computations were made by least squares, giving weights proportional to the square root of  $n$ , the number of stars included in each average (3rd column). Inclusion of brighter stars produced systematic deviations in the lowest most important part of the curve. This may be due to the fact that the relation between  $s-s_0$  and  $H$  is not strictly quadratic. Care was taken that the extent of  $s$ -values occurring in the Milky Way features was well represented by the curve, though stronger densities in black stars might deviate considerably. For all the other plates Table 2 gives only the limit of  $s-s_0$  (3rd column) up to which they have been used in the least-square computation and the mean deviation remaining in the part of the computed reduction curve. The fifth and sixth columns give the same data as in table 2 for the large values not used in the computations.

The values of  $a$  and  $b$  for all plates are contained in Table 5 (p 14.) Expressions with 3rd and 4th powers were tried sometimes, giving in some cases a better representation, but not so much so that it appeared advisable to use them definitely.

TABLE 2a. Data for the reduction-curve of B 3255.

B 3255		22 Ori	P 1
$s-s_0$	$H$	$n$	$O-C$
11.7	18.2	24	+ 0.6
16.3	25.5	17	+ 0.7
23.6	37.8	9	+ 1.2
32.3	51.6	7	+ 0.3
44.8	72.1	8	- 1.4
62.0	104.0	1	- 2.3
73.3	128.6	3	- 0.6
91.3	169.0	3	+ 1.1
115	228	2	+ 5
141	350	3	+ 60

TABLE 2. 1. The Lembang Plates.

Field	Number of Plate	$s-s_0$ (Max)	m. dev.	$s-s_0$	$H$	$n$	$O-C$	$s-s_0$	$H$	$n$	$O-C$
2	3245	101	2.8	181	608	1	- 6				
3	235	128	3.2	155	165	3	+ 23	196	270	3	+ 97
4	3246	71	2.4								
5	233	125	1.8	195	216	3	+ 13	238	352	2	+ 82
6	245	105	2.9	205	280	2	+ 12				
7	3247	40	3.3	191	608	1	+ 83				
8F	3247a	111	1.2	196	291	2	+ 43				
9	239	111	1.8	145	160	2	+ 5	200	243	2	+ 1
10	3248	32	4.4								
11	3249	93	3.7	120	263	1	+ 20				
12	3250	72	1.8	90	132	1	+ 15				
13	261	111	2.6	233	636	1	+237				
14	2404	63	3.8	113	350	2	- 67				
16	2427	48	3.6	111	436	2	+121				
17	3253	94	4.3	165	394	1	- 13				
18	2414	101	3.5								
19	3254	83	4.3	109	251	2	+ 34				
20*	241	91	3.2	142	238	1	- 47				
21*	2460	59	3.7	73	197	3	+ 25				
22	3251	74	4.6	132	370	1	+ 6				
23	2462	43	1.9								
25	98	140	1.0								
26	2420	48	6.7	95	319	5	+ 1				
27	3252	104	3.4								
30	227	147	2.9	215	262	4	+ 64				
32	2447	81	6.5	135	567	3	+137				
34	104	78	3.1	124	260	4	+ 54				
35 C	40	75	2.9	116	222	6	+ 77				
37	2442	97	7.1	134	519	3	+102				
38	2343	102	0.6	142	262	3	- 29				
40	2443	81	5.1	118	402	2	- 26				
41	44	146	3.5	188	263	1	+ 10				
42	48	109	2.1	156	189	3	+ 12				
43	2333	88	2.0	156	292	3	- 18				
44	3260	83	3.7	111	235	1	+ 12	136	321	2	+ 24
45 A	32	63	2.5								
45 B	2451	63	5.8	117	308	1	+ 4				
46	42	63	1.5	182	337	1	+ 14				
47	2340	90	1.8	103	288	1	+ 20	159	777	3	+277
48	2339	113	3.4								
49	2344	77	5.4	134	453	1	+ 85				
50	34	74	4.9								
51	46	72	1.7	167	145	4	+ 16				
52	30	98	7.9								
52 D	38	94	2.3								
52 E	128	84	4.1	123	294	7	+ 48				
53	2335	100	6.0	195	940	2	+471				
54	2347	73	6.1	188	940	2	+485				
55	2349	84	2.5	119	249	2	+ 3	194	501	1	+ 17

Field	Number of Plate	$s-s_0$ (Max)	m. dev.	$s-s_0$	$H$	$n$	$O-C$	$s-s_0$	$H$	$n$	$O-C$
56	3262	100	7.9								
57	3261	91	1.9								
58	3263	104	3.4	155	453	1	+ 16				
59*	2370	98	5.4								
60	2361	101	3.7	124	302	1	+104	148	319	1	+ 75
61	2364	85	1.2	113	217	1	— 21				
62	3264	120	5.2	175	387	1	+ 85				
63	2363	85	4.5	145	295	3	+ 25				
64*	130	88	1.8	114	217	1	+ 40				
65	3265	74	2.3	136	268	2	+ 84				
<b>II. The Boyden Plates.</b>											
15	194	99	1.4	126	159	4	+ 11				
24**	193	123	2.8								
28	197	111	1.5	166	212	4	+ 43				
29	205	85	1.8	164	502	5	+ 96				
31**	2476	121	4.8	182	208	2	+ 49				
32**	207	117	2.2	168	389	2	+134				
33	2479	88	3.5	134	185	4	+ 62				
35	235	108	6.3								
36**	201	56	0.6	131	444	3	+155				
39	209	56	2.7	93	242	2	+ 57	155	538	3	+ 99

## 5. THE EXTRAFOCAL STARDISCS.

*The Lembang plates.* It was intended to take the plates always at the same distance outside the focus, so that they should present discs of the same size. Changes in the original arrangements had to be made, however, after the results of the first measurements. Moreover, because the camera was used for other purposes also, especially variable star work, the focus had to be set anew, often during the same night, for the Milky Way exposures. Hence the size of the discs was not constant and had to be especially investigated.

The discs are circular only in the centre of the plate. Outside the centre they are elliptical, and in an increasing degree so with increasing distance from the centre. Over the region used, where the radial and tangential diameters were measured no indication of cutting off of part of the disc by diaphragms could be found; so we have to assume that always the full aperture works, for the background as well as for the stellar discs. The sizes of the discs are chiefly close to four values, representing one large, one small and two medium types. On 8 plates for each kind the diameters in two directions were measured all over the plate. Their averages for distances 0—5, 5—10, 10—15 mm, etc. from the centre of the plate are represented on the graphs of Fig. 1a p. 9 where crosses represent radial and black dots tangential diameters. For each type they can be represented by quadratic formulae, in which  $d_1$  represents the radial and  $d_2$  the tangential diameter.

$$\begin{array}{ll}
 \text{Large discs} & d_1 = 2.14 - 0.069 r^2, \quad d_2 = 2.14 + 0.008 r^2 \\
 \text{Medium} & \text{,,} \quad 1.90 - 0.064 r^2, \quad 1.90 + 0.009 r^2 \\
 \text{,,} & \text{,,} \quad 1.77 - 0.059 r^2, \quad 1.77 + 0.009 r^2 \\
 \text{Small} & \text{,,} \quad 1.44 - 0.055 r^2, \quad 1.45 + 0.008 r^2
 \end{array}$$

where  $r$  is expressed in cm. The area of the disc is  $\frac{1}{4} \pi d_1 d_2$ .

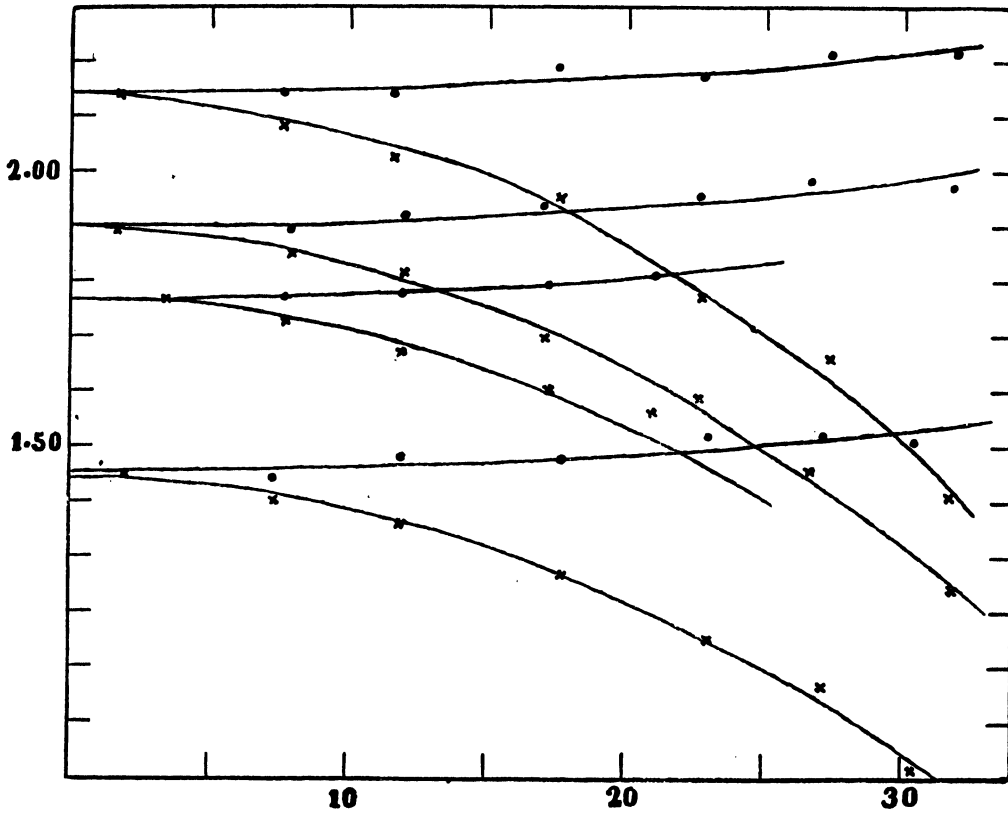


fig. 1a. Diameters of the stardiscs on the Lembang-plates.

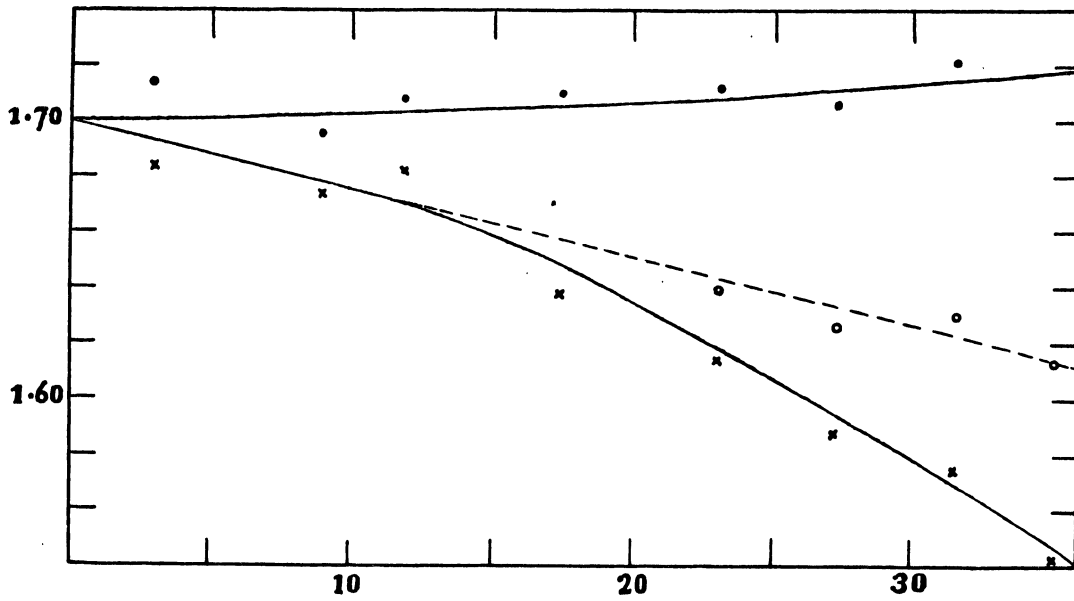


fig. 1b. Diameters of the stardiscs on the Boyden-plates.  
The dashed line represents the radial diameter corrected for silhouetting.

Large	discs	$d_1 d_2 = 4.58 (1 - 0.0295 r^2)$
Medium	„	3.61 (1 — 0.0302 $r^2$ )
„	„	3.14 (1 — 0.0331 $r^2$ )
Small	„	2.10 (1 — 0.0356 $r^2$ )

These expressions represent four mean types; the individual values deviate from them. On all the plates a number of discs in and around the centre have been measured, and reduced to the centre by means of the above data. So for each plate individually the value of the central diameter could be determined. It is given by  $d$  in Table 5.

*The Boyden-plates.* If we arrange the diameter measures of the central stars according to the date of exposure there seem to be slight variations; the differences are so small, however, that we may safely adopt a same law of disc-shape variation over the field for all plates. Adding a constant value to all measured diameters for one plate to reduce them to the curve for central diameter 1.70 mm the averages (crosses for radial and black dots for tangential diameters), shown in Fig. 1b, can be represented by the formula  $d_2 = 1.70 + 0.0017 r^2$  for the tangential diameters. Outside the centre the stellar discs become elliptical at first but after passing 14 mm from the centre the radial diameter becomes silhouetted. Correcting for this effect we obtain the real radial diameter, the dashed line in Fig. 1b, which can be represented by  $d_1 = 1.70 - 0.000246 r$ . The two formulae enable us to compute the variation of the disc-area across the plate.

Date	Centr. Diam.
Jan. 1942	1.721 mm
March 1942	1.657
April 1942	1.702
1946	1.726

## 6. THE LINEAR SCALE OF THE PLATES.

*The Lembang-plates.* The focal distance of the Tessar is 145 mm. The plates were extrafocal so that another distance to the lens, indicated by the same letter  $f$  as the focal distance, determines the linear scale. It was derived by measuring rectangular coordinates of the disc centres of a certain number of stars on plates with different disc sizes. The results deduced for the actual distance  $f$  are collected in Table 3.

TABLE 3. FOCAL DISTANCE (Lembang-plates).

Plate	$d$	$f$	Obs-Form.	$d/f$	$d/f$ ang.
B 2333	2.18	151.59	+ .14	0.0144	0.82
B 2420	1.95	150.56	— .12	0.0130	0.74
B 32	1.71	149.99	+ .11	0.0114	0.65
B 245	1.70	149.83	— .02	0.0113	0.65
B 44	1.43	148.92	— .03	0.0096	0.55

As was to be expected, there is a regular increase of distance  $f$  with disc-diameter  $d$ . It may be represented by  $f = 144.18 + 3.33 d$  or  $d = 0.30 (f - 144.18)$ .

The focal distance 144.2 mm corresponds to the given data. The coefficient 3.33, however, deviates considerably from the aperture ratio 2.7. In the computation of the surface brightness the ratio  $d/f$  is needed. It is given in the 5th column, and can be represented by  $d/f = 0.0100 + 0.0066 (d - 1.50)$ .

The scale of the plates (for  $f = 150$ ) is  $f/57.3 = 2.62$  mm per degree. The distance of 1 mm between the measured points corresponds to  $0^\circ.38$  in the centre; the diameter of the small circle viewed in the Hartmann microphotometer is  $0^\circ.11$ . The diameter of the area measured, viz 50 mm, corresponds to an angular diameter of  $18^\circ.9$ .

*The Boyden-plates.* The Ross-lens has a focal distance of 152.4 mm. All plates were taken outside the focus. The actual focal distance of 4 plates was determined (Table 3a). The differences in diameter are too small to compute a reliable formula for the focus as a function of the diameter. For further reduction it is sufficient to adopt a mean focal distance of 162.5 mm for all Boyden-plates. For the computation of  $d/f$  we distinguish three groups of plates with different  $d$ . The plates of January 1942 and 1946 have a mean  $d$  of 1.723 (4 plates), the March 1942-plates (5 plates) have  $d = 1.657$ , and for the last plate  $d = 1.702$ . The corresponding  $d/f$ -values become 0.01060, 0.01020 and 0.01047. The diameter of the area measured 60 mm, corresponds to an angular diameter of  $20^{\circ}.9$ .

TABLE 3a. FOCAL DISTANCE (Boyden-plates).

Plate	$d$	$f$
2479	1.72	162.80
193	1.72	162.86
207	1.66	162.06
209	1.66	162.36

## 7. THE INTENSITY DISTRIBUTION ACROSS THE STARDISCS.

The stardisks are seen to be surrounded by a darker borderring, while also the central part is slightly darker than the intermediate parts. In consequence of this uneven distribution of intensity across the disc the intensity measured in the centre is not exactly equal to the mean surface intensity computed from the total light and the area of disc. In order to determine the ratio between central and mean intensity we had to measure the variation of intensity along the radius of the disc. This was done first with the Hartmann microphotometer by setting the circular opening at consecutive points of a diameter. Afterwards the Moll microphotometer was used, which registers the variation of density as a curve, of which as many points can be read as are needed (See fig. 2). Since the relative intensityprofile turns out to be the same for bright as for faint stars, the increase of intensity towards the edge of the disc is considered real and not due to Eberhard effect. For deriving intensities the reduction formula  $H = as + b(s-s_0)^2$  of section 4 was used.

*The Lembang-plates.* In Table 4 the intensities, expressed in the central density = 100, are given for every 0.1 of the radius for a number of measured circular discs.

TABLE 4. DISTRIBUTION OF INTENSITY ACROSS THE STELLAR DISCS. (Lembang-Plates).

Number in Uran. Arg.	Sp.	0.1	0.2	0.3	0.4	0.5	0.6	0.7	0.8	0.9	$\alpha$	Min.	$d$
28 Oph	B 0	96	85	76	71	71	74	87	127	145	1.11	0.46	1.89
28 Aql	B 3	99	95	90	83	81	83	93	106	118	1.00	0.49	1.89
16 Pyx	A 0	100	98	94	87	78	74	82	94	108	1.13	0.59	2.14
53 Sco	A 0	99	96	91	87	85	84	87	99	114	1.06	0.59	1.85
11 Aqi	A 0	99	94	92	87	84	84	94	109	115	1.04	0.54	1.70
90 Oph	A 2	96	87	79	73	70	72	79	103	133	1.02	0.52	2.14
193 Oph	A 2	99	95	90	82	76	77	86	100	117	1.10	0.54	2.15
168 Sco	A 2	99	92	85	80	78	85	98	110	118	0.99	0.50	1.40
135 Oph	F 0	99	94	88	84	82	85	94	103	107	1.03	0.48	1.45
215 Vel	G 0	98	97	91	86	82	80	87	106	133	0.97	0.58	1.90
136 Sgr	K 0	98	95	91	85	79	74	73	85	108	1.09	0.68	2.16
92 Lib	K 0	98	92	86	80	76	73	75	85	120	1.09	0.64	1.86

From these results the ratio  $\alpha$  of the central to the mean intensity may be deduced. It seems to be slightly dependent on the size  $d$  of the disc. Adding to them the values derived from the elliptical discs on the same plates we have as averages for large, medium and small discs:

$d =$	2.15 mm	1.83 mm	1.41 mm
$\alpha =$	1.077	1.041	1.003

which may be represented by a linear function

$$\alpha = 1.061 + 0.100 (d-2.0)$$

From approximate values a first expression  $\alpha = 1.053 + 0.095 (d-2.0)$  had been derived and was used in some of the reductions; the difference is negligible.

Furthermore it appears from Table 4 that the distribution of intensity across the disc depends on the spectral type. By mere visual inspection it was at once clear that for the red stars the dark ring which surrounds the disc is sharp and black, for white stars less dark but broader. So it was possible, with but few exceptions to recognize the spectrum by simple inspection of the appearance of the discs, at least to distinguish between early and late spectral types. In the intensity curves which can be constructed from Table 4 this difference presents itself in a different distance, in unit radius, of the intensity minimum from the centre. For this distance, given under "Min" in Table 4, the averages are, for 2 B-stars 0.48, for 7 A-stars 0.54 and for 3 G—K-stars 0.63. For the factor  $\alpha$ , we have after reduction by the above formula to  $d = 2.0$ : for B—A (9 stars) 1.068, for F—K (10 stars) 1.055; so there is no clear difference and the same value of  $d$ , only dependent on disc size, may be assumed for all the stars on a plate.

*The Boyden-plates.* In table 4a some data for the Boyden-plates are collected. A mean value of 0.88 for  $\alpha$  is found from 17 stars of all spectral types. For the B and A-stars 0.90 and for the later types 0.86 is found for the mean  $\alpha$ . In general the dark outer rings of the discs are blacker than those of the Lembang-plates, so that a faint star is often clearly seen as a ring only, bordering an even disc not measurably blacker than the surrounding background. The position of the minimum intensity on the disc as a function of spectral type is nearly the same as found for the Lembang-plates, viz. 0.52 for the B- and A-type stars and 0.65 for the G- and K-stars.

TABLE 4a. DISTRIBUTION OF INTENSITY ACROSS THE STARDISCS (Boyden-plates).

Plate	Number in Uran. Arg.	Sp.	0.1	0.2	0.3	0.4	0.5	0.6	0.7	0.8	0.9	$\alpha$	Min.
207	40 Cru	B 1	99	100	100	98	96	94	98	118	218	0.83	0.60
193	107 Car	B 5	100	100	97	94	94	101	107	130	200	0.80	0.45
207	39 Cru	B 8p	100	96	95	94	92	95	98	113	169	0.91	0.51
201	20 TrA	B 8	100	99	95	90	83	84	91	113	198	0.88	0.52
2479	69 Mus	B 9	100	100	98	91	90	91	98	112	165	0.96	0.50
2476	1 Mus	A 0	98	99	98	95	86	80	81	109	189	0.96	0.63
209	28 Nor	A 2	100	97	97	95	97	99	108	138	212	0.81	0.40
2476	17 Mus	G 5	101	99	97	93	88	87	88	96	170	0.93	0.60
205	11 Mus	K 0	100	100	100	100	100	100	98	109	167	0.84	0.70
205	257 Car	K 0	100	98	97	94	94	94	92	109	200	0.83	0.66
207	22 Cru	K 2	100	97	94	90	84	81	82	90	164	0.95	0.63
209	13 Ara	K 5	100	100	96	96	91	85	89	112	251	0.89	0.64



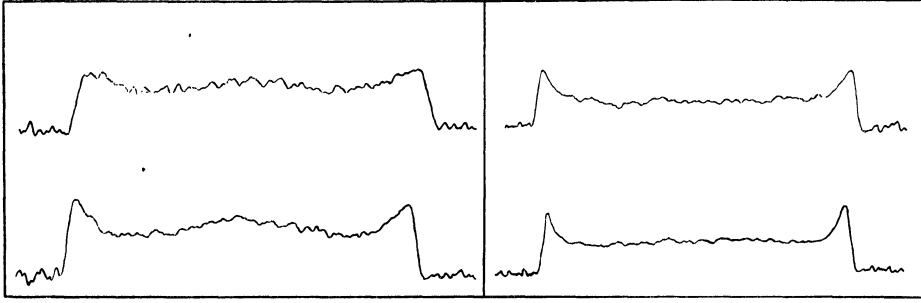


fig. 2. Density distribution along the radius of the star disc. The upper tracings are of B-stars, the lower ones of K-stars. The registrations on the left have been obtained from Lembang-plates, on the right from Boyden-plates.

## 8. THE LIMITING MAGNITUDE OF THE STARS.

In Publication 3 of the Amsterdam Institute the limiting magnitude of the stars was derived by determining the percentages of stars, in each 0.1 of a magnitude, visible on the plates. The magnitude for which the percentage was 50, was defined as the limiting magnitude. As already remarked, the faint photographic magnitudes in the Draper-catalogue are bad, and moreover not complete, so that this method did not work very well. The strong black rings of the late type stars, moreover, caused the limiting magnitude to be a function of spectral type. Since the limiting magnitude is not used in the reductions, it suffices to know that, for the Lembang-plates, the limit of visibility was between 8.5 and 9.0 magn. and for the Boyden-plates between 9.0 and 9.5.

## 9. REDUCTION FORMULAE FOR SURFACE BRIGHTNESS.

The brightness of a star  $H$  (in unit  $10^m$  star, hence  $H = 10^{0.4(10-m)}$ ) is spread out on the plate over a disc of diameter  $d$ , area  $\frac{1}{4}\pi d^2$ , or, more generally, over an ellipse with diameters  $d_1$  and  $d_2$ , area  $\frac{1}{4}\pi d_1 d_2$ . Expressed in square degrees this area is  $\frac{1}{4}\pi d^2 (57.3/f)^2$ , hence the mean surface brightness, in unit one  $10^m$  star per sq.d., is

$$h = \frac{4}{\pi} \left( \frac{f}{57.3 d} \right)^2 H.$$

The area of the discs decreases with increasing distance to the centre in ratio  $d_1 d_2 / d^2$ . This fact has been taken approximately into account by multiplying the surface brightness used in Section 4 in deriving the constant  $a$  and  $b$  by a factor  $\delta$  the average of  $d^2 / d_1 d_2$  over the measured part of the plate. This factor is derived from Fig. 1 by integrating  $d_1 d_2$  over the consecutive rings of the measured region around the centre. So  $\delta$  is found to be 1.135 for the large and 1.102 for the small discs of the Lembang-plates and 1.025 for the Boyden-plates. To find the surface intensity in the centre of the disc the result has to be multiplied by  $\alpha$ , the ratio of central to mean intensity. For the reduction curves for intensity for each plate formulae  $H = as + b(s-s_0)^2$  have been derived, hence

$$h = \frac{4}{\pi} \left( \frac{f}{57.3 d} \right)^2 \delta \alpha (as + b(s-s_0)^2) = C_1 s + C_2 (s-s_0)^2$$

The factors with which the coefficients  $a$  and  $b$  must be multiplied to get  $C_1$  and  $C_2$  depend on the size  $d$  of the discs. For the Lembang-plates with central diameter

$$d = 2.20 \ 2.10 \ 2.00 \ 1.90 \ 1.80 \ 1.70 \ 1.60 \ 1.50 \ 1.40 \ 1.30 \text{ they are}$$

$$\log \frac{C_1}{a} = \log \frac{C_2}{b} = 0.337 \ .372 \ .408 \ .447 \ .490 \ .536 \ .586 \ .640 \ .697 \ .759 \text{ and for the Boyden plates with}$$

$$d = 1.72 \ 1.70 \ 1.66 \text{ they are}$$

$$\log \frac{C_1}{a} = \log \frac{C_2}{b} = 0.311 \ 0.319 \ 0.337$$

In this way the coefficients  $C_1$  and  $C_2$ , given in Table 5, have been derived from  $a$  and  $b$ .

TABLE 5. REDUCTION FACTORS FOR THE PLATES.  
(The Lembang-plates).

Field	Central Star	$a$	$100 b$	$s_0$	$d$	$C_1$	$100 C_2$
1	22 Ori	1.451	0.425	47	1.81	4.46	1.30
2	BAC 2306	1.705	0.932	66	1.76	5.50	3.00
3	60 Ori	0.470	0.285	51	1.45	2.18	1.32
4	18 Mon	1.683	0.820	67	1.75	5.47	2.67
5	$\kappa$ Ori	0.632	0.211	28	1.50	2.77	0.92
6	7 Mon	1.057	0.122	68	1.67	3.75	0.43
7	$\delta_1$ CMi	1.616	0.578	59	1.78	5.11	1.83
8	101 Mon	2.443	0.751	66	1.76	7.83	2.41
9	$\nu_3$ CMa	0.689	0.260	68	1.48	3.09	1.17
10	154 Mon	3.231	2.204	49	1.75	10.47	7.14
11	176 CMa	0.828	0.997	90	1.78	2.62	3.16
12	269 Pup	0.933	0.404	70	1.77	2.97	1.29
13	$\sigma$ CMa	1.087	0.268	90	1.49	4.83	1.19
14	$\xi$ Pup	1.334	1.500	105	1.92	3.67	4.13
16	$\eta$ Pyx	1.417	1.286	96	2.14	3.23	2.93
17	$r$ Pup	1.208	0.761	61	1.73	4.02	2.53
18	$\epsilon$ Pyx	1.269	0.285	61	1.90	3.55	0.80
19	159 Pup	1.106	0.814	57	1.78	3.50	2.58
20*	$\lambda$ Vel	0.566	1.130	66	1.48	2.54	5.06
21*	F Vel	1.785	0.781	103	2.17	3.96	1.73
22	M Vel	0.827	1.465	79	1.77	2.64	4.69
23	31 Ant	1.254	0.198	60	2.20	2.73	0.43
25	$s$ Vel	0.431	0.144	94	1.49	1.92	0.64
26	J Vel	1.671	1.982	74	1.94	4.53	5.37
27	9 Cen	1.117	0.361	46	1.74	3.68	1.19
30	$\delta$ Cen	0.534	0.175	53	1.48	2.38	0.78
31	17 Mus	0.719	0.284	110	1.47	3.27	1.29
32	$\beta$ Cru	1.432	1.300	89	1.90	4.00	3.63
34	$\xi_2$ Cen	1.087	0.518	50	1.50	4.71	2.24
35C	V Cen	0.838	0.350	79	1.43	4.03	1.68
36	$\epsilon$ TrA	1.545	0	—	1.43	7.36	0
37	$l$ Lup	1.254	1.394	54	1.92	3.44	3.82
38	59 Lup	1.079	0.686	86	1.90	3.02	1.92
40	e Lup	1.482	1.797	55	2.15	3.35	4.06
41	$\eta$ Nor	0.529	0.434	80	1.43	2.54	2.08
42	$\epsilon_2$ Ara	0.470	0.289	73	1.44	2.21	1.36
43	$h$ Lup	0.898	0.698	73	2.18	1.98	1.54

Field	Central Star	$a$	100 $b$	$s_0$	$d$	$C_1$	100 $C_2$
44	$\nu$ Lib	1.291	0.648	65	1.78	4.06	2.04
45 A	$\zeta$ Sco	0.770	1.082	63	1.70	2.65	3.73
45 B	$\eta$ Sco	0.898	1.456	87	1.91	2.49	4.04
46	$\vartheta$ Sco	0.552	0.671	86	1.42	2.69	3.27
47	67 Sco	1.617	0.959	105	1.89	4.56	2.70
48	$\omega_2$ Sco	0.965	0.329	95	1.92	2.65	0.90
49	134 Sco	2.449	0.224	44	2.13	5.61	0.51
50	$\eta$ Sgr	1.159	0.302	61	1.42	5.64	1.47
51	24 Oph	0.485	0.172	69	1.42	2.34	0.83
52	X Sgr	0.672	1.188	80	1.42	3.26	5.77
52 D	44b Oph	0.747	0.558	77	1.42	3.60	2.69
52 E	X Sgr	1.292	0.583	55	1.46	5.94	2.69
53	$\zeta$ Oph	1.194	0.622	101	1.90	3.36	1.75
54	$\eta$ Oph	2.412	0	39	2.14	5.41	0
55	$\lambda$ Sgr	1.173	0.683	93	1.90	3.28	1.91
56	32 Sgr	1.074	0.860	87	1.76	3.44	2.76
57	$\mu$ Oph	1.047	0.797	51	1.77	3.33	2.54
58	117 Sgr	1.048	1.145	79	1.76	3.37	3.69
59*	2H Sct	1.606	0.429	71	1.90	4.48	1.19
60	68 Oph	1.320	0.224	66	2.18	2.92	0.50
61	20 Aql	0.936	1.036	83	1.94	2.54	2.81
62	5 Aql	1.375	0.201	76	1.77	4.39	0.64
63	72 Oph	1.002	0.600	64	2.15	2.27	1.36
64*	$\nu$ Aql	0.874	0.594	43	1.44	4.13	2.81
65	$\vartheta$ Ser	1.357	0.005	56	1.78	4.27	0.02
The Boyden-plates							
24**	$a$ Car	0.581	0.210	151	1.72	1.80	0.65
15	$\pi$ Pup	0.580	0.473	189	1.72	1.80	1.46
28	M Car	0.593	0.256	186	1.66	1.99	0.88
36**	$\varepsilon$ TrA	0.840	1.047	132	1.66	2.83	3.54
29	18 Mus	1.143	0.822	161	1.64	3.84	2.76
32**	$\beta$ Cru	0.570	0.565	186	1.66	1.92	1.92
39	33 TrA	0.728	1.363	153	1.66	2.46	4.58
35	$\beta$ Cen	1.605	1.300	173	1.70	5.10	4.15
31**	17 Mus	0.516	0.285	165	1.72	1.59	0.90
33	67 Mus	0.726	0.140	179	1.72	2.27	0.44

## 10. REDUCTION TO THE CENTRE OF THE PLATE.

The density of the silver deposit decreases towards the edge of the plate because of the diminishing surface illumination by inclined light pencils. This illumination of the tangential plane diminishes, from geometrical relations, as  $\cos^3 \varphi$  if  $\varphi$  denotes the angle of incidence upon the plate. Added to it are the effects of the elliptical cross section of the inclined pencil (as  $\cos \varphi$ ) and of the absorptions and reflections in the optical system.

*The Lembang-plates.* The amount of the decrease of surface intensity as a function of the distance to the centre may be determined by two different methods. Firstly by measuring this decrease on plates exposed to uniformly luminous surface; secondly by comparing the common parts of two adjacent plates

taken in such a way that the centre of one corresponds to a border region of the other. For the first method the Milky Way plates themselves may be used if the effect of the unequal brightness of the regions photographed can be eliminated. We may expect this elimination to take place in the average of a number of plates, if those with the brightest cloud forms are left out, and plates with brighter regions in the centre are averaged with such as have the brighter regions at the borders.

For the law of intensity-decrease towards the border of the plate we assumed  $h/h_{\text{centre}} = \cos^n \varphi$ . Since, in the absence of intensity-marks on these plates we are not able to construct a characteristic curve giving the relation between  $h$  and  $s$  we have assumed  $h$  to be simply proportional to  $s$  in this range of values; then we may use the same expression for the decrease of silver densities toward the border. So for each ring between the consecutive circles at 5,10,15 . . . mm around the centre the average  $s$  was derived for a number of plates. On these plates also a number of points were measured outside the part used for galactic intensity, in order to find the law of decrease with more certainty.

TABLE 6. DECREASE OF INTENSITY WITH DISTANCE FROM CENTRE.  
( $\log s(c) - \log s$  in 0.001)

Field Nr	5—10	10—15	15—20	20—25	25—30	30—35	$d$
3	— 3	— 12	0	+ 41	+ 65	+134	1.45
5	— 15	— 7	+ 13	47	99	185	1.49
9	— 2	+ 26	63	122	156	222	1.40
13	+ 21	43	80	104	134	183	1.48
20*	+ 7	12	36	62	88	156	1.48
35 C	— 1	+ 4	22	38	71	153	1.41
51	+ 6	32	59	96	134	227	1.37
52	+ 22	+ 6	18	48	81	146	1.38
52 D	— 2	— 1	+ 6	38	76	140	1.45
6	— 6	+ 4	23	49	66	126	1.66
14	+ 34	67	98	142	177	257	1.92
18	+ 18	36	83	128	143	234	1.90
37	+ 25	36	62	95	126	180	1.88
38	+ 34	35	52	91	132	220	1.86
47	— 2	+ 19	41	64	85	137	1.85
48	+ 37	77	110	149	186	245	1.89
53	+ 18	40	59	91	103	151	1.90
16	+ 17	14	52	77	129	193	2.13
21*	0	2	37	80	104	164	2.19
23	+ 4	33	52	79	143	230	2.19
40	+ 15	39	87	155	182	262	2.14
43	+ 5	3	33	79	102	136	2.20
54	+ 17	35	76	112	182	265	2.13
60	+ 43	80	113	160	200	276	2.13
63	+ 9	28	65	134	186	269	2.13
	004	011	033	066	100	172	1.43
	020	039	066	101	127	194	1.86
	014	029	064	109	154	224	2.15
Mean	.012	.026	.054	.091	.126	.196	
$\Delta \log \sec \varphi$	.00048	.00142	.00287	.00468	.00669	.00882	
19.5 $\Delta \log \sec \varphi$	.009	.028	.056	.091	.130	.172	

In Table 6 the plates have been arranged in three groups, for small, medium and large sizes of the discs. It gives the decrease of intensity in successive rings, relative to the central circle, in the form of the logarithm of the ratio of central  $s$  to the ring value. It shows this logarithmic decrease to vary with the disc size, being largest for the great discs. On the Heidelberg-plates of the Northern Milky Way just the reverse was found, viz a far stronger variation on three plates with small discs. The values given in the table are strongly affected by the mean density in the small central circle, which is rather uncertain depending as it does on few points only in a small area which may have a large chance deviation. Since, moreover, no direct cause for a dependence on disc size can be indicated, it seemed advisable to assume one general reduction to the centre for all plates. Comparing the logarithmic differences with the mean  $\log \sec \varphi$  for each of the rings, we find a linear relation (only the outermost ring deviates)  $\log s = n \log \sec \varphi$  with  $n$  about 20, or more precisely 19.5, which may be used as an empirical reduction formula.

Another method to find the reduction to centre is the intercomparison of adjacent plates. According to the program of plate centres as given on p. 2 the centres of adjacent plates, situated at the same latitude, are  $10^\circ$ , at different latitudes  $11^\circ.2$  distant from one another. Since the measured area is a circle of  $19^\circ$  diameter, the centre of each plate, on the mean, is slightly outside the limit of the measured part of an adjacent one. So they have a large segment in common, one half of which is nearer to one, the other half nearer to the other centre. The same mean factors for reduction to centre  $f_c$  and  $f_b$  hold for the central and the border half of the common segment on both plates. If we call  $A_c$  and  $A_b$  the mean intensity of these parts on plate  $A$ , and  $B_c$  and  $B_b$  on plate  $B$ , after reduction to centre then in the absence of other errors these values should only show a constant plate difference:  $A_c + D = B_b$ ;  $A_b + D = B_c$ . If, however, the reduction to centre is erroneous and corresponds to another power of  $\sec \varphi$ , hence should the ratio  $f_b/f_c$  be  $p$  times larger, then we have

$$A_c + D = pB_b \quad \text{and} \quad B_c - D = pA_b$$

Then the constant plate difference and the factor  $p$  (supposed constant, because  $f_b$  and  $f_c$  for all these pairs of plates are nearly the same) may be found from the four averages of reduced intensities:

$$D = \frac{1}{2}(B_c + B_b - A_c - A_b); \quad p = (A_c + B_c):(A_b + B_b)$$

In this way the intercomparison of plates affords a control of the values adopted after the discussion in the preceding paragraph. If these values are right the mean result for  $p$  should be found to be 1; else these data give a correction to the assumed reduction.

TABLE 7. COMPARISON OF ADJACENT PLATES.

Plate		$B_b - A_c$	$B_c - A_b$	$D$	wgt	$\log p$
$B$	$A$					
3	1	- 150	- 130	- 140	2	+ 022
4	2	+ 2	- 1	0	2	- 001
4	3	+ 241	+ 249	+ 245	1	+ 007
5	1	- 177	- 169	- 173	1	+ 010
5	3	- 30	- 22	- 26	2	+ 016
6	3	+ 154	+ 158	+ 156	2	+ 004
6	4	- 82	- 80	- 81	2	+ 001
6	5	+ 175	+ 177	+ 176	2	+ 002
7	2	- 19	- 19	- 19	1	000
7	4	- 16	- 8	- 12	2	+ 004
8	4	+ 47	+ 84	+ 66	2	+ 008
8	6	+ 151	+ 194	+ 172	2	+ 020
8	7	+ 129	+ 146	+ 138	1	+ 008

Plate		$B_b - A_c$	$B_c - A_b$	$D$	wgt	log $p$
$B$	$A$					
8 F	3			+ 64	1	
8 F	4	- 195	- 172	- 184	1	+ 009
8 F	5	+ 101	+ 101	+ 101	1	000
8 F	6	- 85	- 92	- 88	2	+ 003
8 F	7			- 145	1	
8 F	8	- 307	- 261	- 284	3	
9	5	+ 121	+ 135	+ 128	1	+ 022
9	6	- 41	- 47	- 44	1	- 005
9	8	- 355	- 394	- 374	1	- 018
9	8 F	+ 43	+ 39	+ 41	1	- 004
10	7	+ 239	+ 247	+ 243	1	+ 004
10	8	+ 74	+ 33	+ 54	2	- 014
10	8 F	+ 410	+ 399	+ 404	1	- 005
11	8	- 310	- 343	- 326	2	- 017
11	9	- 11	- 15	- 13	1	- 003
11	10	- 345	- 412	- 378	3	- 009
12	10	- 332	- 287	- 310	3	+ 024
12	11	+ 29	+ 30	+ 30	1	+ 002
13	9	+ 231	+ 225	+ 228	1	- 004
13	11	+ 278	+ 261	+ 270	1	- 009
14	11	+ 191	+ 190	+ 190	1	- 001
14	12	+ 130	+ 122	+ 126	1	- 005
14	13	- 66	- 111	- 88	2	- 018
15	13	- 106	- 99	- 102	2	
15	14	- 1	- 22	- 12	1	
16	12	+ 137	+ 133	+ 135	1	- 003
16	14	+ 20	+ 6	+ 13	2	- 007
17	14	- 157	- 158	- 158	1	- 001
17	15	- 171	- 173	- 172	1	
17	16	- 121	- 128	- 124	1	- 004
18	16	- 50	- 51	- 50	3	000
18	17	+ 94	+ 70	+ 82	1	- 018
19	15	- 168	- 157	- 162	2	
19	17	- 17	+ 7	- 5	2	- 021
20*	17	- 65	- 65	- 65	2	000
20*	18	- 119	- 97	- 108	1	+ 021
20*	19	- 31	- 38	- 34	1	- 006
21*	19	+ 249	+ 236	+ 242	2	- 008
21*	20*	+ 239	+ 255	+ 247	2	+ 010
22	20*	+ 26	+ 33	+ 30	3	+ 007
22	21*	- 209	- 202	- 206	1	+ 004
23	18	- 43	- 26	- 34	2	+ 017
23	20*	+ 52	+ 39	+ 46	2	- 014
23	22	+ 21	+ 21	+ 21	1	000
24**	20*	+ 80	+ 71	+ 76	1	
24**	21*	- 177	- 191	- 184	2	
24**	22	+ 31	+ 18	+ 24	2	
25	22	- 2	- 15	- 8	2	- 012
26	22	+ 110	+ 108	+ 109	2	- 001
26	24**	+ 136	+ 132	+ 134	2	
26	25	+ 88	+ 127	+ 108	3	+ 029

Plate		$B_b - A_c$	$B_c - A_b$	$D$	wgt	log $p$
$B$	$A$					
27	22			- 42	1	
27	25	- 21	- 6	- 14	4	+ 017
27	26	- 133	- 109	- 121	3	+ 018
28	24**	+ 99	+ 79	+ 89	2	+ 013
28	26	- 26	+ 1	- 12	2	
29	26	+ 202	+ 213	+ 208	1	
29	28	+ 271	+ 213	+ 242	3	+ 025
30	25			- 57	1	
30	26			- 163	1	
30	27	- 51	- 50	- 50	3	+ 001
30	29	- 460	- 453	- 456	1	
31	28	+ 61	+ 48	+ 54	3	
31	29	- 176	- 222	- 199	5	
31**	28	- 75	- 60	- 68	3	- 009
31**	29	- 325	- 310	- 318	5	- 008
31**	31	- 129	- 153	- 141	5	
32	29	- 247	- 214	- 230	3	
32	30	+ 187	+ 214	+ 200	3	+ 021
32	31	- 24	- 10	- 17	2	+ 006
32	31**	+ 116	+ 97	+ 106	1	
32**	29	- 279	- 261	- 270	3	- 004
32**	30	+ 189	+ 187	+ 188	3	
32**	31	- 55	- 66	- 60	2	
32**	31**	+ 61	+ 62	+ 62	2	000
32**	32	- 40	- 9	- 24	5	
33	29	- 191	- 155	- 173	3	- 013
33	31	+ 24	+ 4	+ 14	3	
33	31**	+ 159	+ 159	+ 159	3	000
33	32	+ 59	+ 60	+ 60	3	
33	32**	+ 82	+ 103	+ 92	3	- 009
34	30	+ 170	+ 147	+ 158	3	- 023
34	32	- 37	- 34	- 36	3	+ 002
34	32**	- 53	- 31	- 42	3	
35	31**	+ 710	+ 736	+ 723	1	- 004
35	32	+ 619	+ 590	+ 604	3	
35	32**	+ 603	+ 641	+ 622	3	- 009
35	33	+ 514	+ 548	+ 531	3	- 009
35	34	+ 674	+ 657	+ 666	2	
35 C	32	+ 16	- 28	- 6	1	- 024
35 C	32**	- 20	- 19	- 20	1	
35 C	33	- 109	- 70	- 90	1	
35 C	34	+ 70	+ 50	+ 60	1	- 014
35 C	35	- 589	- 596	- 592	4	
36	33	- 89	- 79	- 84	1	
36	35	- 609	- 573	- 591	2	
36	35 C	+ 39	- 23	+ 8	1	- 033
36**	33	- 33	- 1	- 17	2	
36**	35	- 552	- 514	- 533	2	- 013
36**	35 C	+ 65	+ 40	+ 52	1	
36**	36	+ 27	+ 45	+ 36	5	
37	34	- 42	- 54	- 48	2	- 012

Plate		$B_b - A_c$	$B_c - A_b$	$D$	wgt	log $p$
$B$	$A$					
37	35	- 706	- 686	- 696	1	
37	35 C	- 102	- 98	- 100	2	+ 001
38	35	- 657	- 640	- 648	2	
38	35 C	- 50	- 87	- 68	3	- 025
38	36	- 83	- 76	- 80	2	+ 004
38	36**	- 116	- 113	- 114	3	
38	37	+ 24	+ 23	+ 24	2	- 001
39	36	+ 34	+ 10	+ 22	3	
39	36**	+ 10	0	+ 5	3	+ 004
39	38	+ 91	+ 80	+ 86	2	
40	35 C	- 132	- 131	- 132	1	000
40	37	- 43	- 40	- 42	2	+ 003
40	38	- 59	- 41	- 50	2	+ 015
41	38	- 61	- 65	- 63	3	- 003
41	39	- 183	- 183	- 183	2	
41	40	- 35	- 38	- 36	2	- 002
42	36*	- 230	- 232	- 231	1	
42	39	- 257	- 240	- 248	3	
42	41	- 56	- 60	- 58	3	- 003
43	40	- 41	- 31	- 36	2	+ 011
43	41	+ 9	- 10	0	1	- 019
44	43	+ 138	+ 151	+ 144	2	+ 013
45 A	41	- 23	- 25	- 24	2	- 002
45 A	42	+ 21	+ 32	+ 26	2	+ 011
45 A	43	- 24	- 23	- 24	1	+ 002
45 B	41	+ 30	+ 10	+ 20	1	- 018
45 B	42	+ 68	+ 69	+ 68	2	000
45 B	45 A	+ 41	+ 40	+ 40	4	- 001
46	42	+ 76	+ 61	+ 68	1	- 015
46	45 A	+ 56	+ 23	+ 40	3	- 030
46	45 B	+ 13	- 23	- 5	4	- 029
47	43	+ 385	+ 359	+ 372	1	- 016
47	44	+ 231	+ 202	+ 216	2	- 014
47	45 A	+ 401	+ 392	+ 396	1	000
48	44	- 12	- 21	- 16	2	- 007
48	47	- 220	- 232	- 226	2	- 006
49	45 A	+ 54	+ 73	+ 64	3	+ 018
49	45 B	+ 19	+ 39	+ 29	3	+ 017
49	46	+ 42	+ 36	+ 39	2	- 005
49	47	- 339	- 353	- 346	2	- 007
50	45 B	+ 104	+ 101	+ 102	1	- 003
50	46	+ 124	+ 92	+ 108	2	- 020
50	49	+ 20	- 6	+ 7	1	- 014
51	47	- 347	- 358	- 352	2	- 006
51	48	- 127	- 114	- 120	2	+ 013
51	49	- 22	- 23	- 22	2	- 001
52	49	- 33	- 36	- 34	3	- 002
52	50	- 82	- 83	- 82	2	- 001
52	51	+ 38	+ 23	+ 30	1	- 014
52 D	47	- 268	- 279	- 274	1	- 005
52 D	49	+ 51	+ 57	+ 54	3	+ 004



<i>B</i>	Plate <i>A</i>	$B_b - A_c$	$B_c - A_b$	<i>D</i>	wgt	log <i>p</i>
52 D	51	+ 94	+ 79	+ 86	3	— 013
52 D	52	+ 71	+ 44	+ 58	4	— 020
53	48	+ 134	+ 135	+ 134	1	+ 001
53	51	+ 281	+ 267	+ 274	2	— 011
54	51	+ 71	+ 92	+ 82	3	+ 022
54	52	+ 15	+ 16	+ 16	1	+ 001
54	52 D	— 23	— 1	— 12	3	+ 017
54	53	— 176	— 191	— 184	3	+ 013
55	50	— 47	— 38	— 42	2	+ 005
55	52	— 8	+ 57	+ 24	2	+ 037
55	52 D	— 91	— 55	— 73	1	+ 022
56	52	+ 62	+ 56	+ 59	3	— 004
56	52 D	+ 17	+ 19	+ 18	3	+ 001
56	54	+ 24	+ 25	+ 24	1	+ 001
56	55	+ 32	+ 84	+ 58	3	+ 031
57	53	— 216	— 223	— 220	1	— 005
57	54	— 55	— 16	— 36	3	+ 038
57	56	— 77	— 73	— 75	2	+ 003
58	55	+ 51	+ 31	+ 41	3	— 013
58	56	+ 11	— 5	+ 3	2	— 009
59*	55	+ 163	+ 195	+ 179	1	+ 018
59*	56	+ 79	+ 73	+ 76	3	— 004
59*	57	+ 96	+ 114	+ 105	3	+ 016
59*	58	+ 117	+ 106	+ 112	2	— 006
60	57	+ 25	+ 25	+ 25	1	— 009
60	59*	— 42	— 36	— 39	1	+ 006
61	58	— 44	— 41	— 42	3	+ 003
61	59*	— 149	— 162	— 156	2	— 008
62	59*	+ 40	+ 35	+ 38	3	— 002
62	60	+ 106	+ 105	+ 106	2	— 001
62	61	+ 151	+ 171	+ 161	3	+ 013
63	60	— 75	— 64	— 70	3	+ 012
63	62	— 175	— 180	— 178	1	— 004
64*	61	— 12	— 14	— 13	3	— 002
64*	62	— 144	— 156	— 150	2	— 009
65	60	— 12	— 12	— 12	1	000
65	61	+ 45	+ 54	+ 50	1	+ 008
65	62	— 121	— 102	— 112	3	+ 014
65	63	+ 62	+ 64	+ 63	2	+ 002
65	64*	+ 59	+ 44	+ 52	1	— 013

In Table 7 the results of the comparison of all the pairs of plates are contained; the last column gives the values of  $\log p$ . It is seen that as a rule they are small, and their average is nearly zero. So both methods confirm one another in giving the same reduction to the centre. Owing to the difference of focal distances of the Lembang- and the Boyden-plates, the  $f_b$ 's (resp.  $f_c$ 's) for two such adjacent plates are not identical, moreover the exponent  $n$  may be different for the two series of plates; therefore  $\log p$  is not computed in those cases. Also if the overlapping field was too small to be divided into two halves, the  $\log p$  was omitted.

*The Boyden-plates.* The reduction to the centre could not be made by the first method as most plates contain strong starclouds. Therefore, for the derivation of  $n$ , the second method was used in a some-

what modified form. Adopting as before  $h = h_{\text{centre}} \cos^n \varphi$  and  $H = as$ , we obtain the densities  $s_1$  and  $s_2$  of the same part of the sky on two adjacent plates, for which the formula  $n \log \cos \varphi_1 / \cos \varphi_2 = \log s_1 / s_2 + \text{constant}$  holds. By taking as many points as possible the exponent  $n$  may be derived as the slope of the straight line representing this formula. Comparing the plates 201—209, 2479—2476 and 193—197 we find  $n = 10.8, 10.4, 11.2$  resp.

A less reliable method, a modification of the first method, was also tried. All  $s$ -values measured on a plate were plotted against their distances from the plate-centre. The cloud of points in such a plot shows no sharp upper boundary, owing to the strong and irregular starclouds. But the lower boundary is sharply depicted, suggesting an equal sky illumination over the whole plate. A curve, laid through the lowest points may give a rough value of  $n$ . For plate 194, 209, 201, 2479, 2476, and 193 we found

$$n = 11.6, 10.4, 13.5, 11.5, 17.8 \text{ and } 16.4.$$

The first series for  $n$  being more trustworthy, we finally adopt  $n = 11$  for the reduction of all the plates.

On the Boyden-plates standardization marks have been impressed. At our request Dr. Paraskevopoulos kindly sent us the values of the constants of the standardizing photometer. The characteristic curves of two plates, derived by means of these marks, show that for the parts used here  $s$  varies nearly as  $h^2$ , so that  $n = 11$  for the decrease of blackness towards the border of the plates corresponds to a  $n = 5$  for the intensity decrease. This may also explain the high exponent  $n = 19.5$  found in the case of the Lembang-plates. Since the enlargement of the spherical surface by projection on the tangential plane is as  $\cos^3 \varphi$  the remaining  $\cos^2 \varphi$  may be ascribed to absorptions, reflections and other effects of oblique course of the light through the optical system. Only in the brightest starclouds, where different parts of the characteristic curve come into play, differences of some tens in our intensity scale on this account may occur. For an exact photometry of the brightest galactic clouds a special investigation by means of special plates well standardized will be required, where all the sources of small systematic errors can be eliminated which are unavoidable in a first photometric survey of the entire Milky Way such as the present one.

## 11. REDUCTION OF THE INTENSITIES TO ONE SYSTEM.

Thus the method of reduction of the measurements on the plates was as follows. The measured silver densities  $s$  were reduced, by means of the formulae on page 13 and the constants  $C_1$  and  $C_2$  of Table 5 (derived from the characteristic curve data of Table 5) to apparent intensity. By means of the data of Table 6, expressed in a formula for the reduction to centre, true intensities  $h$  were deduced, expressed in unit one  $10^m$  star per square degree. Since in Section 4 the constant  $as_0$  was omitted for  $H$  a corresponding zero point correction is required for each plate. So they now have to be reduced to one common system by means of constant corrections.

These corrections can be derived by means of the differences between adjacent plates shown on the areas they have in common. Each adjacent pair of plates affords a difference, averaged from all the separate values; by their combination the reductions to one system may be effected. For the northern galactic zone this was done after all the plates had been finished, by smoothing all the plate differences over the entire material in one solution of all the unknown corrections. For the southern galactic zone this was not possible. Owing to the circumstances mentioned in Section 1 the plates nearest to the South pole were not at hand, when all the other ones were finished. They form the connecting link between the preceding and the following parts nearer to the equator. So we could not make one discussion of all plates and plate-differences, but had to proceed in parts. First the two groups between  $180^\circ$  and  $240^\circ$  ("Puppis-section") and between  $300^\circ$  and  $360^\circ$  ("Scorpio-section") of longitude had to be treated separately, to be combined with the middle part  $240^\circ$ — $300^\circ$  ("Centaurus-section") afterwards. This is a less satisfactory procedure, as for the limiting plates of each group, that have neighbours only to one side, the interconnection is lacking and the weight

is smaller. Because it happened that plate P 15 was also lacking in the Lembang work, the Puppis-section was composed by P 1 — 14, P 16—23. The Scorpio-section consisted of P 37, 38, 40—65, and the remaining plates formed the Centaurus section. For the reduction of the Centaurus-section plates P 12—46 overlapping with the Puppis- and Scorpio-sections were used to obtain a smooth connection with the other sections.

The zero-point of the definite system of intensities for the southern region should be as far as possible identical with the zero point of the northern system. To accomplish this two methods were tried. First the isophotes 2 of the visual Milky Way, as traced on the Milky Way Maps in Annalen Lembang Vol. II, part 1. were copied on the maps, representing for each plate all the intensity results at the exact place and containing at the same time all the visible stars. If we may assume that in the visual observations the adaptation of the northern and southern parts was accomplished satisfactorily, the scale value 2 in one and in the other part must represent the same intensity. So for each plate we are able to fix its zero-point. Another way is available by proceeding from the regions near the equator where the northern and the southern program overlap. There the plate differences between plates of the northern and of the southern program allow to adapt the latter to the system of the former.

Both ways have been followed in a combined derivation of the individual plate corrections. The data are given in Tables 7 and 8. Table 7 gives the results of the intercomparison of pairs of adjacent plates, which were treated in the preceding paragraph. The differences  $B_b - A_c$  and  $B_c - A_b$  are given separately, their mean is the difference  $D$  (the attached weight depends on the number of comparisons, i.e. the common area which itself depends on the distance of the two centres). The  $\log p$  in the last column increases with the difference between the two values for  $B-A$ .

The reduction to a common zeropoint, which was first finished for the Scorpio-section, was made by successive approximations. The visual isophote 2 was taken to correspond to the intensity 130, as in the northern part (cf. Publ. Amst. 3, p. 31). The mean intensity values along this isophote on the different plates were all larger, so that corrections had to be subtracted. These negative corrections are given in Table 8, second column, together with their weights. The next column gives the value of these corrections deduced from the comparison with the intensities of the Northern Milky Way (Publ. Amsterdam 3). These are the data that will not change in the successive approximations. Proceeding from the isophotic values of column 2 the differences  $D$  (Table 7) of a plate with each of the adjacent plates give additional values; their averages are given for each plate, as derived from each section, in columns 4, 5, 6 of Table 8, together with their weights.

TABLE 8. CORRECTIONS TO THE PLATES (All negative).

1	2	3	4	5	6	7
Plate	From Is. 2	From North. M.W.	From Plate comparison			Corr. adopt.
			Puppis Section	Centaurus Section	Scorpio Section	
1		157 5	160 1½			173
2	298 3	298 5	286 3			297
3	15 3	18 4	42 4			34
4	298 4	294 6	304 7			298
5		+2 2	6 4½			13
6	190 3		221 6½			204
7	243 3		281 5½			265
8	431 4		416 10½			414
8 F	129 3		111 10½			115
9	148 2		142 5			141
10	498 5		487 8			491

1	2	3	4	5	6	7
Plate	From Is. 2	From North. M.W.	From Plate comparison			Corr. adopt.
			Puppis Section	Centaurus Section	Scorpio Section	
11	132 4		122 10½			119
12	134 3		174 7	164 4		156
13	422 3		399 3½	394 3		394
14	316 5		280 6	289 5		295
15				303 4		289
16	249 4		285 5	274 4		266
17	133 4		127 8	130 5		131
18	190 1		176 6	181 4		204
19	120 3		108 5	107 3		111
20*	67 5		72 11	74 7		71
21*	334 4		332 5	329 4		327
22	100 4		100 5	101 7		102
23	100 ½		132 5	120 4		129
24**	149 3			116 5		125
25	81 3			85 5		87
26	183 3			216 7		206
27	71 3			65 4		73
28	203 3			202 5		203
29	447 3			451 8		452
30	24 4			17 7		19
31	253 5			260 6		258
31**	130 3			123 4		127
32	221 4			224 9		221
32**	220 4			200 9		201
33	280 2			292 9		285
34	167 3			167 6		168
35	814 5			820 10		817
35 C	222 4			214 10		219
36	232 4			226 6		231
36**	275 4			268 7		268
37	99 2			121 5	126 4	118
38	149 6			151 8	134 4	152
39	262 4			261 5		262
40	87 2			88 5	93 8	96
41	74 3			77 7	84 12	77
42	42 5			34 6	35 8	29
43	49 3			61 5	67 5	63
44	195 2			198 2	195 4	211
45 A	59 5			53 7	56 15	54
45 B	113 6			99 6	101 12	97
46	117 3			94 5	95 14	91
47	418 3				445 10	436
48	206 1				188 5	200
49	123 6				123 19	121
50	175 3				194 10	176
51	68 5				78 13	75
52	126 6				105 16	105
52 D	164 5				171 18	164

1	2	3	4	5	6	7
Plate	From Is. 2	From North. M.W.	From Plate comparison			Corr. adopt.
			Puppis Section	Centaurus Section	Scorpio Section	
53	297 1				323 6	334
54	133 6				148 11	146
55	138 2				114 14	113
56	180 6				169 15	170
57	85 2				105 10	110
58	168 3				150 9	149
59*	220 5				238 13	232
60	121 2				134 11	143
61	94 5				91 12	92
62	237 6	239 30			248 14	243
63	63 5	69 20			65 6	69
64*	92 5	80 30			84 8	82
65	136 6	145 40			131 10	142

In these and further approximations the relative weights of the data of different origin must be taken into account. Neglecting first the differences of weight within one kind of data, we may call  $\mu_1$  the mean error of an isophote result and  $\mu_2$  the m.e. of a plate pair difference. From the intercomparison of the two halves of the common segments a value  $\mu_2 = 9$  was found; but this is likely to be too low, because it depends on two very near areas, and larger deviations may be expected from more remote parts. In the results of which Col. 4—6 give the averages, both errors are contained in the same way, hence their m.e. is  $\sqrt{\mu_1^2 + \mu_2^2}$ . Comparing the result of Col. 4—6 (average of  $n$  values) with column 2, we have differences with a m.e.  $\sqrt{\mu_1^2 + \frac{1}{n}(\mu_1^2 + \mu_2^2)}$ . Thus both  $\mu$  could be found; the result was  $\mu_1 = 10$  and  $\mu_2 = 23$  for the Scorpio region. A system of weights for the Puppis- and Scorpio-regions based on these values was adopted, running up from 1 to 6 for the isophote data, according to the extension and the character of the isophotic curves on the plates. For the plate differences  $D$  the weights were 1 to 4. The Centaurus-section gave  $\mu_1 = 11$  and  $\mu_2 = 18$ . A slightly different system of weights was then used for this region.

The averages of the values of column 2, 3 and 4—6 constituted a second approximation for the corrections; new values for column 4—6 were derived from them; and so further successive approximations were made till they did not change any more. The final results as contained in the last column now of course are different from the means of columns 2—6.

In Publication 3, p. 34 we found by mutual comparison of several plates in the Scutum-region differences in the scale of intensity. Empirical scale-corrections were applied to reduce the intensities to mean values. In the same way comparison of the brightest parts in Sagittarius now showed that constant plate corrections are not sufficient to ensure a homogeneous system. The different scales probably are due to imperfections in the formulae assumed for the characteristic curves. Since we cannot be sure which of them is the best or the right one, we have adopted a scale according to the average of the 6 Lembang-plates that contain the Sagittarius cloud. Of plate 52E only half was measured. For each of them a correction of the form factor  $\times$  (Int — 300) was derived to reduce all the intensities above 300 in the Sagittarius region.

For	P 49	P 50	P 52D	P 52E	P 52	P 55	the factor
is	+ 0.45	— 0.15	+ 0.09	+ 0.15	— 0.18	+ 0.19	

Large scale differences were found in the region of galactic longitude  $250^\circ$  and latitude  $-5^\circ$  covered by the Lembang-plate 2420 (P 26) and the Boyden plates 193 and 197 (P 24 and P 23). Extinction cannot explain these differences between Boyden-plates 193 and 197, since these plates were taken at about the same altitude.

Nor is the reason to be found in the imperfection of only the brightest part of the characteristic curve, for the differences occur also in the lowest intensity values. The following linear corrections had to be applied for reduction to a mean intensity scale:

Plate 197 Corr. =  $-0.25$  (Int—160) for intensity larger than 160

Plate 193 Corr. =  $+0.56$  (Int—167) for intensity larger than 167

Plate B 2420 Corr. =  $-0.16$  (Int—182) for all intensities.

As in Publ. 3, the intensities corrected in this way, will be taken as the final values, to be used in the next chapter.

## 12. THE FINAL RESULTS.

The results of the plates, after they had been reduced to one system by applying the constant corrections and, for some brightest part, the linear scale corrections, were collected on large scale maps ( $1^\circ=3$  cm), drawn after the galactic coordinates of the stars computed by A. Marth (Monthly Not. **53**, p. 74, 384) based on a galactic pole  $190^\circ, +30^\circ$ . By means of an episcopes the image of each separate plate with all its final intensity values was projected upon this map; because of the difference between the cylindrical projection of the map and the tangential projection of the plates only small parts could at the same time be brought into coincidence by means of the surrounding stars. In this final discussion the data of plates 31 and 36 were omitted, because the same fields were covered by the Boyden-plates 31\*\* and 36\*\*.

The final results are presented here in two ways. Firstly by condensing the separate values into averages. The surface brightness of the Milky Way background deduced from centres of faint stars, by subtracting the intensity of this star, received only half weight, since they appeared to deviate more than other values. Results of all the plates covering a region were included as much as possible into each average. Usually a total weight of 5 or 6, corresponding to the number of determinations, was aimed at for each intensity value. In the more crowded regions weights up to 12 occur; only at the outer parts, where few plates can be combined and the separate values are more thinly spread, weights smaller than 5 are found. On the final charts I—XV, also based on Marth's coordinates, these averages are given in black print, in two figures only, the hundreds being indicated by different printing type. The smallest type 00-99 represents the values below 100, the next larger ones in italics *00-99* the values 100—199, followed by 00-99, **00-99**, **00-99**, **00-99** representing values of 200—299, 300—399, 400—499, 500—599. <sup>1)</sup> Two dots behind the number denote a weight  $1-2\frac{1}{2}$ , one dot refers to a weight  $3-4\frac{1}{2}$ , whereas the others have greater weight. Where in border regions the averages depend on intensities from one plate only, the result is given in parentheses.

As a second form of the final results isophotic curves were constructed for each full number of tens in the intensity. These isophotes are independent of the method of averaging just mentioned; they were drawn using the separate values on the large-scale maps. These values, however, had to be corrected beforehand in an empirical way owing to systematic differences between the plates. In the discussion of the Heidelberg plates it had been found that after the application of the constant zero point corrections the intensities of the separate plates did not always correspond. Especially towards the borders of the measured parts systematic differences, gradually changing over the plate appeared to be present. They must be ascribed partly to the influence of atmospheric irregularities, extinction and skylight, but chiefly to variations of sensitivity across the plate, differences in development and other irregular photographic effects.

The same is the case with the southern plates, but in a still stronger degree. A large number of plates had to be rejected and repeated because they showed an irregular yellowish tinge; and it may be that some of the plates measured had them in a lesser degree, though at inspection they did not show irregularities. Such differences will produce sudden jumps in the resulting average intensities at the circles limiting the plates (i.e. their measured areas), and thus may considerably distort the isophotes and the shape of galactic

<sup>1)</sup> On the charts I - XV the figures actually are 0.6 times smaller than those given in the text.

objects. In order to eliminate them, intensity differences from the mean intensity as derived from all plates were computed for each plate. With their signs reversed they were considered as corrections needed to reduce the single plate intensities to the mean of all the plates. They were smoothed out by means of curves of constant differences drawn across the plate. By transferring these curves upon the large-scale maps and correcting the intensity values it was possible to draw the isophotes with the confidence that the galactic objects were well represented, whereas the mean intensity in each region was not changed thereby. Of course, the absolute values of intensity may somewhat fluctuate from one region to another, as they are based on the average of continually varying groups of plates.

Often the drawing of the isophotes was a difficult and uncertain matter because of the remaining local and accidental differences between the plates. It is clear that, since the isophotes are affected by chance errors of the measured intensity values, no stress should be laid on minor details in their shapes, which may not be real. There was a tendency to smooth out the minor fluctuation of an amount comparable with the mutual differences, believing them to be due to such chance errors. Comparison, however, with the photographic pictures of Barnard and the beautiful Milky Way Atlas of Ross, showed that they mostly correspond to real small scale features of the Milky Way and had to be considered as the image of these features smoothed out by extrafocality. It even happened that an isolated strongly deviating value first was omitted as erroneous and afterwards appeared to coincide with a real small dark or bright spot. So for deciding on the reality of details we let ourselves be guided mostly by a careful comparison with those photographic pictures. The same was necessary where in bright regions crowded with stars the measured points were too thinly spread to decide which of them should be connected into one feature. Since in Ross' Atlas the southern parts beyond  $40^\circ$  of southern declination are lacking — its completion for the entire circumference of the Milky Way must be considered as a most urgent task of celestial photography — we could first only avail ourselves of the small-scale photographs of S. J. Bailey (Harvard Annals 72, No. 3) as comparison pictures. Afterwards, through the kindness of Father F. J. Heyden S. J. of Georgetown College Observatory we could make use of contact prints of a series of plates of the Southern Milky Way, taken with the same instrument as used by Ross but with shorter exposure time; they were extremely helpful in our comparisons. The amount of detail, represented by the measured intensities on the plates, thus is shown to be richer than was originally supposed, and it exceeds by far the results of visual observations.

On the charts I—XV, these isophotes, going up in steps of 10, are represented in red lines, the lines for multiples of 50 being heavier. For the brightest parts only the heavier lines for multiples of 50 are drawn, because they would be too much crowded. The same is done in regions with many bright stars, where the measured points are more scarce and the form of the objects cannot be well ascertained from them. Where owing to large gaps in the system of measured points the course of the isophotes was uncertain, dotted lines give their hypothetical shapes. To reproduce all the details of the isophotes, a larger scale of the maps than was used for the Northern Milky Way, is needed for the galactic longitudes  $242^\circ$  to  $10^\circ$ . For the remaining longitudes a scale identical with the northern charts appeared to be sufficient. The stars are inserted in red colour also, as well as the coordinate points for every  $5^\circ$  of equatorial coordinates which are marked by crosses.

It must be remarked that isophotes and intensity numbers deviate from their true values around the bright stars, since the plates had not been backed, so that smoothed halos surrounding these stars were produced. In the Northern Milky Way such an increased intensity was shown around  $\alpha$  Aurigae. In these southern parts many bright stars show such high intensities around them, the most excessive in the case of Sirius, where a circle of  $1.5^\circ$  radius could not be measured and excess intensity is perceived up to a distance of  $5^\circ$ , or even more.

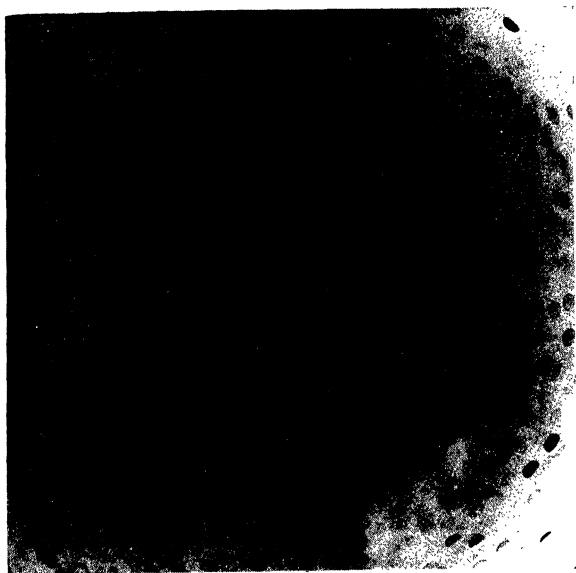
The mean error of the intensity values on the large-scale maps shows strong differences owing to varying quality of the plates. The best plates, showing entirely clear borders, are the Boyden-plates 31\*\*

and 33 taken in 1946. Comparing the individual intensity measures on these two plates in the overlapping region a mean error of 8 units in the intensity interval 100—400 is found for a single measure. The other Boyden-plates, taken during the war, often show veiled unexposed film, an indication that old plates had to be used. The empirical reductions to the mean of the plates show that in this case the quality is certainly not better than the Lembang-plates. Comparing intensity means in the intensity interval 100—300 derived from 3 values on the Lembang-plates of the fields 35C, 32 and 34 with corresponding ones of the Boyden-plates for 32\*\*, 29\*\* and 36\*\*, we derive a mean error of the mean of 3 measurements of 8 units. Most figures on the printed charts I—XV are means of 6 individual measurements. Assuming this region as representative for the whole Southern Milky Way, the mean error of a figure on these charts is then roughly 6 units in the interval just mentioned. Judging from the empirical intensity corrections, especially for higher intensities, the mean error may locally be much larger.

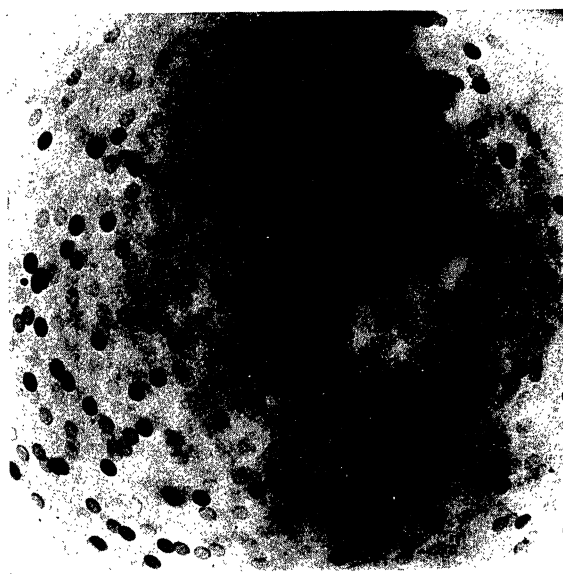
The system of isophotes on the charts I—XV gives a numerical representation of the distribution of surface intensity in the Galactic zone. In order to get an idea as to what this system of curves stands for, a drawing in shades was made of two adjacent parts of the most variegated region between  $310^\circ$  and  $10^\circ$  of longitude. A reproduction (Plate II) is added to the present work. A comparison with the visual representations of the Milky Way (e.g. the *Uranometria Argentina* and "Die Südliche Milchstrasse" in *Annalen Lembang II*, part 1) shows at once what far greater wealth of detail is offered by the photographic method. We might describe the picture as the aspect the Milky Way would present to eyes that were far more sensitive to faint glares of light than ours and at the same time able to distinguish smaller details. A comparison with the focal photographs of Barnard and Ross shows a smoothing out of all sharp detail, thus gaining a true representation of the surface intensity which is lacking there.



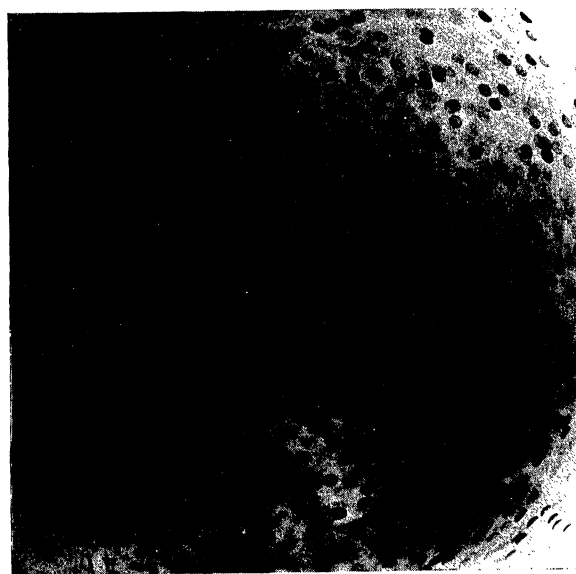
1



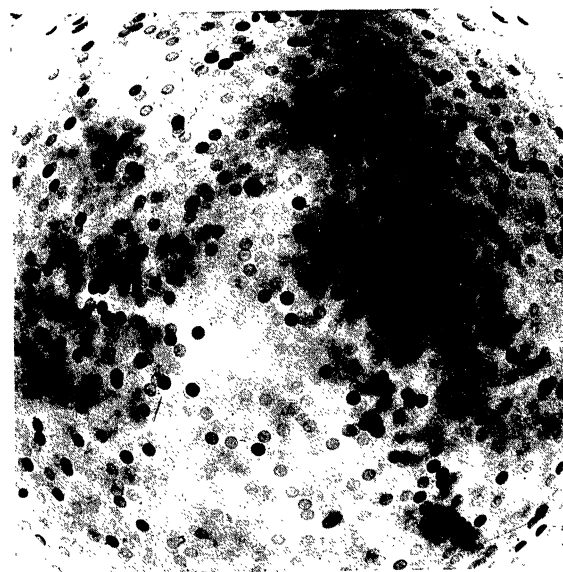
2



3



4



1. B 2428  $\alpha_1$  Centauri  
3. B 48  $\epsilon$  Arae

2. B 2447  $\beta$  Crucis  
4. B 30 X Sagittarii

The diameter of the measured circular region is 0.88 of the side of the square.

Plate II

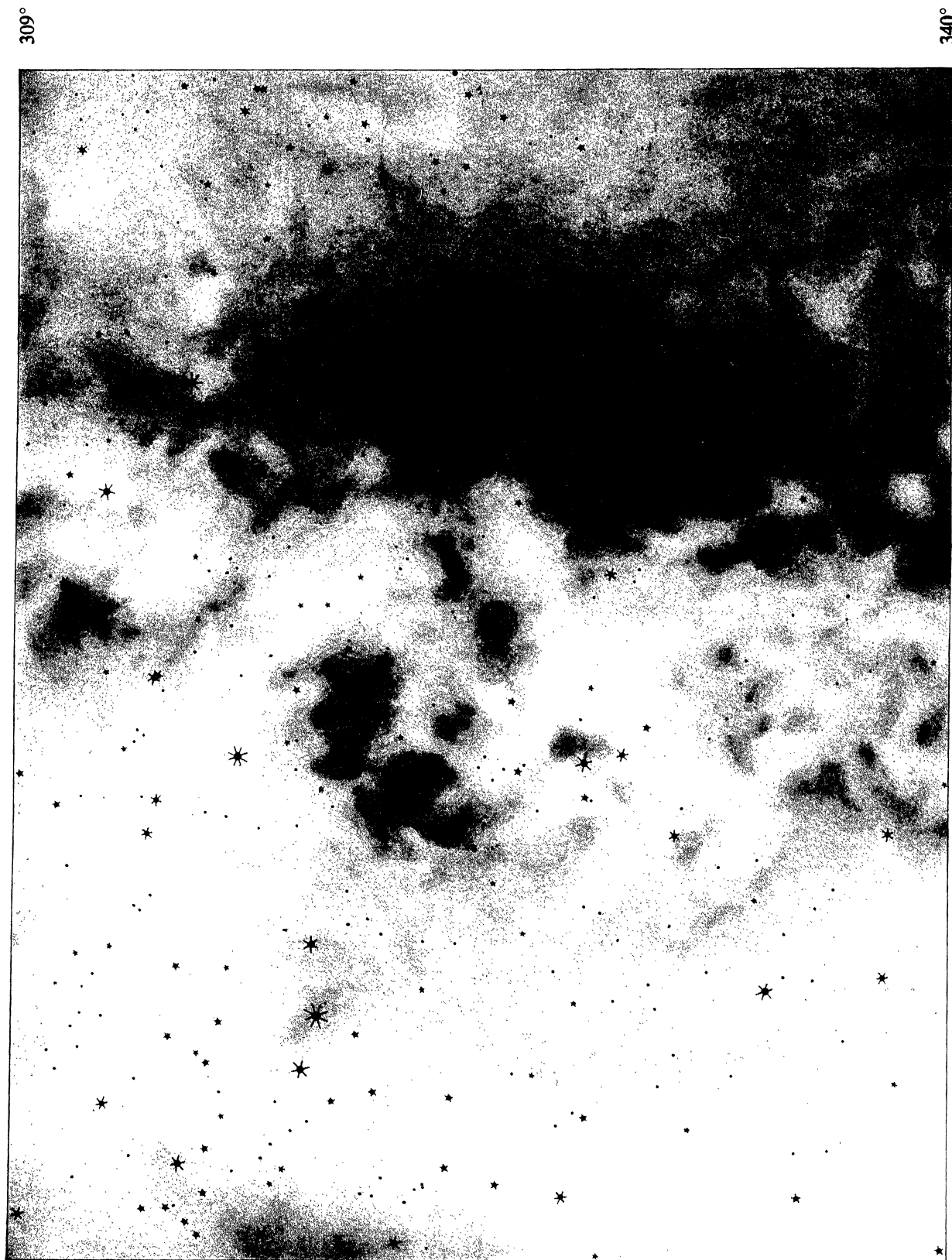
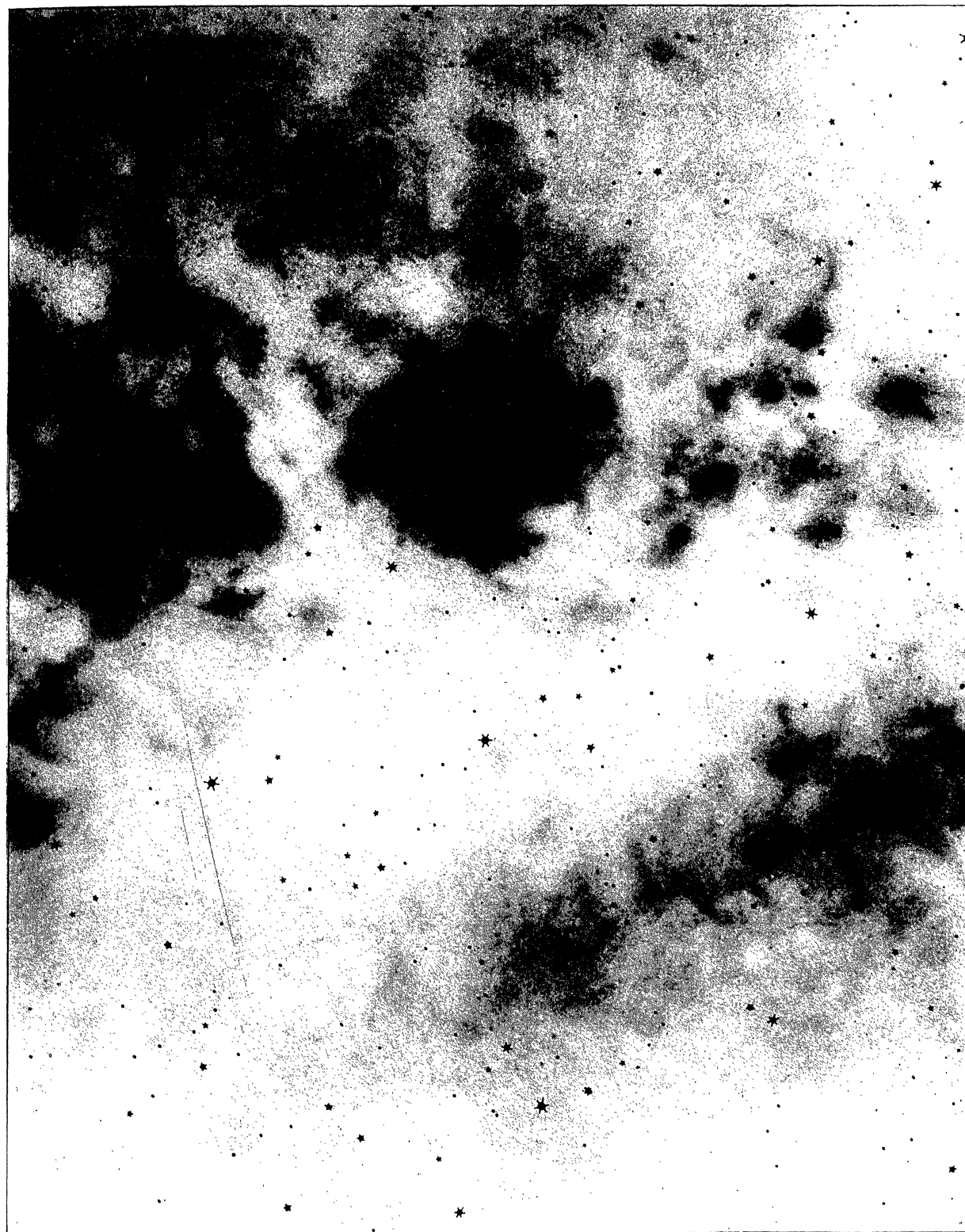


Plate III

339°



10°

